Framing Pyramids

Minh N. Do, *Member, IEEE*, and Martin Vetterli, *Fellow, IEEE*

***Abstract*— In 1983, Burt and Adelson introduced the Laplacian pyramid (LP) as a multiresolution representation for images. We study the LP using the frame theory, and this reveals that the usual reconstruction is sub-optimal. We show that the LP with orthogonal filters is a tight frame, and thus the optimal linear reconstruction using the dual frame operator has a simple structure that is symmetric with the forward transform. In more general cases, we propose an efficient filter bank for the reconstruction of the LP using projection that leads to a proved improvement over the usual method in the presence of noise. Setting up the LP as an over-sampled filter bank, we offer a complete parameterization of all synthesis filter banks that provides perfect reconstruction for the LP. Finally, we consider the situation where the LP scheme is iterated and derive the continuous-domain frames (framelets) associated with the LP.**

***Index Terms*— Laplacian pyramid, frames, filter banks, multiresolution signal processing, pseudo inverse, projection, wavelets, framelets.**

I. Introduction and Motivation

Multiresolution data representation is a powerful idea. It captures data in a hierarchical manner where each level corresponds to a reduced-resolution approximation. One of the early examples of such a scheme is the Laplacian pyramid (LP), proposed by Burt and Adelson [1] for image coding. The basic idea of the LP is the following. First, derive a coarse approximation of the original signal, by lowpass filtering and downsampling. Based on this coarse version, predict the original (by upsampling and filtering) and then calculate the difference as the prediction error. Usually, for reconstruction, the signal is obtained by simply adding back the difference to the prediction from the coarse signal. The process can be iterated on the coarse version. Analysis and usual synthesis of the LP are shown in Figure 1(a) and 1(b), respectively.

A drawback of the LP is implicit oversampling. Therefore, in compression applications it is normally replaced by subband coding or wavelet transform which is a critically sampled scheme and often an orthogonal decomposition. However, the LP has the advantage over the critically sampled wavelet scheme that each pyramid level generates only one bandpass signal, even for multidimensional cases. This property makes it easy to apply many multiresolution algorithms using a coarse-to-fine strategy [2] to the LP. Furthermore, the resulting bandpass signals of the LP do not suffer from the "scrambled" frequencies as in the critical sampling scheme. The reason for this frequency scrambling effect is illustrated in Figure 2 for the 1-D case. As can be seen, the highpass channel is folded back into the low frequency after downsampling, and thus its spectrum is reflected. In the LP, this effect is avoided by downsampling the lowpass channel only. Therefore, the LP permits further subband decomposition to be applied on its bandpass images. A possible scheme is a pyramidal decomposition where the bandpass images of the LP are fed into directional filter banks [3]. The final result is a set of directional subband images at multiple scales [4], [5].

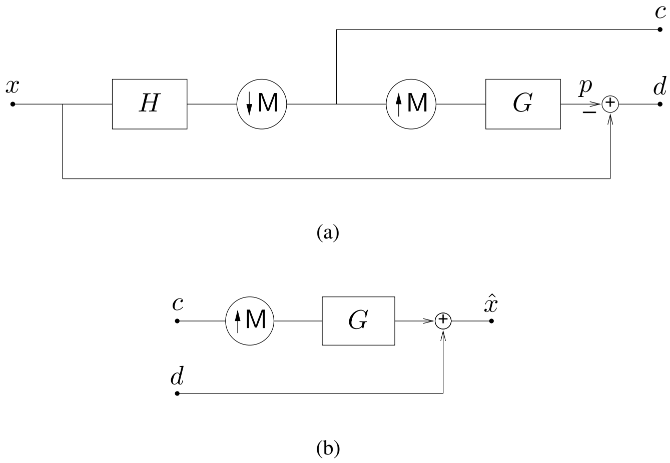

Fig. 1. Laplacian pyramid scheme. (a) Analysis: the outputs are a coarse approximation c and a difference d between the original signal and the prediction. The process can be iterated by decomposing the coarse version repeatedly. (b) Usual synthesis.

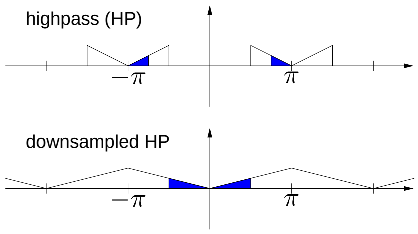

Fig. 2. Illustration of the "frequency scrambling" in 1-D due to downsampling of the highpass channel. *Upper*: spectrum after highpass filtering. *Lower*: spectrum after downsampling. The filled regions indicate that the high frequency is folded back into the low frequency.

For many applications like compression and denoising, the coefficients in the transform domain are processed further, and this can introduce errors due to quantization or thresholding. The processed coefficients are then used to reconstruct the

M. N. Do was with the Audiovisual Communications Laboratory, Department of Communication Systems, Swiss Federal Institute of Technology, Lausanne, Switzerland. He is now with the Department of Electrical and Computer Engineering, the Coordinated Science Laboratory, and the Beckman Institute, University of Illinois, Urbana IL 61801- (email: minhdo@uiuc.edu).

M. Vetterli is with the Audiovisual Communications Laboratory, Department of Communication Systems, Swiss Federal Institute of Technology, Lausanne, Switzerland, and with the Department of Electrical Engineering and Computer Science, University of California, Berkeley CA 94720 (email: martin.vetterli@epfl.ch).

This work was supported in part by a Ph.D. Fellowship from the Department of Communication Systems, EPFL, and the Swiss National Science Foundation under Grant 21-52439.97.

original data. For the LP, the usual reconstruction algorithm – adding the prediction from the coarse version with the difference, produces a perfectly reconstructed signal in the absence of noise, but turns out to be usually suboptimal otherwise.

Because the LP is an overcomplete representation (there are more coefficients after the analysis than in the input), it must be treated as a *frame* operator. Frames are generalizations of bases that lead to redundant expansions. A key observation is that one should use the *dual frame* operator for the reconstruction. While this seems a somewhat trivial observation, it has not been used in practice, probably because the usual reconstruction, while suboptimal, is very simple. Yet, we will show that gains around 1 dB are actually possible over the usual reconstruction. Beyond this improvement, we also believe that a full treatment of what is one of the most standard image processing structure is probably worthwhile in its own right, be it only for pedagogical reasons.

Recently, there have been a considerable interest in wavelet and filter bank frames [6], [7], [8], [9], where the greater design freedom available by the overcomplete systems leads to a variety of attractive features over bases. The LP frame offers a simple scheme that has low computation complexity (there is only one filtering channel), can be easily extended to higher dimensions (e.g. via separable extension), and has small redundancy (even in higher dimensions).

The outline of the paper is as follows. In Section II, we introduce the notation and set up the operators for the LP using both the time-domain and the polyphase-domain representations. The dual frame operator or the pseudo inverse is defined together with its properties for reconstruction. In Section III, we consider the LP with orthogonal filters and show that it is a *tight frame*, and thus the pseudo inverse has a simple structure which is symmetrical with the forward transform. In Section IV, inspired by the structure of the pseudo inverse for the tight frame LP, we propose a new reconstruction for more general LP's that leads to better performance compared to the usual method. In Section V, by setting up the LP as an oversampled filter bank (FB), we find a parameterization for all synthesis FB's providing perfect reconstruction for the LP. The oversampled FB view of the LP leads to a study of iterated LP and its associated continuous frames, so called framelets, in Section VI. We conclude in Section VII with some discussions.

II. PRELIMINARIES

A. Signals, Operators and Notations

Since the LP is valid for signals in any dimension and often used for images, we use multi-dimensional notation for generality. A d-dimensional discrete-time signal is a sequence of real-valued numbers defined on the integer lattice $\mathbb{Z}^d$, e.g. $x[n],\ n \in \mathbb{Z}^d$. Signals with finite energy belong to a Hilbert space $l_2(\mathbb{Z}^d)$ with the inner product defined as $\langle x, y\rangle = \sum_{n\in\mathbb{Z}^d} x[n]y[n]$, and thus the l_2-norm is $\|x\| = \sqrt{\langle x, x\rangle} = \sqrt{\sum_{n\in\mathbb{Z}^d} x[n]^2}$. The z-transform of a d-dimensional signal $x[n]$ is denoted by

$$X(z) = \mathcal{Z}\{x[n]\} \stackrel{\text{def}}{=} \sum_{n\in\mathbb{Z}^d} x[n]z^{-n}.$$

where raising a d-dimensional complex vector $z = (z_1, \ldots, z_d)^T$ to a d-dimensional integer vector $n = (n_1, \ldots, n_d)^T$ yields $z^n = \prod_{i=1}^d z_i^{n_i}$. On the unit hyper-sphere, $z = e^{j\omega} \stackrel{\text{def}}{=} (e^{j\omega_1}, \ldots, e^{j\omega_d})^T$, $X(e^{j\omega})$ is the Fourier transform of $x[n]$. For a matrix in the z-domain with real coefficients $\mathsf{A}(z)$, denote $[\mathsf{A}(z^{-1})]^T$ by $\mathsf{A}^*(z)$. On the unit hyper-sphere, $\mathsf{A}^*(e^{j\omega})$ is the transpose conjugation of $\mathsf{A}(e^{j\omega})$.

The sampling operation is represented by a $d\times d$ nonsingular integer matrix M [10]. For an M-fold downsampling, the input $x[n]$ and the output $x_d[n]$ are related by

$$x_d[n] = x[\mathsf{M}n].$$

For an M-fold upsampling, the input $x[n]$ and the output $x_u[n]$ are related by

$$x_u[n] = \begin{cases} x[k] & \text{if } n = \mathsf{M}k,\ k \in \mathbb{Z}^d \\ 0 & \text{otherwise.} \end{cases}$$

In the z-domain, the upsampling operation can be simply written as $X_u(z) = X(z^{\mathsf{M}})$. The quantity z^{M} is defined to be a vector whose k-th element is given by z^{m_k}, where m_k is the k-th column of the matrix M. We denote $|\det(\mathsf{M})|$ by $|\mathsf{M}|$.

B. Burt and Adelson's Laplacian Pyramid

The structure of the Laplacian pyramid is shown in Figure 1. We concentrate first on one level of the LP; multilevel LP's are discussed later. The filtering and downsampling operation for the LP shown in Figure 1(a) yields the coarse approximation signal

$$c[n] = \sum_{k\in\mathbb{Z}^d} x[k]h[\mathsf{M}n - k] = \langle x, \tilde{h}[\cdot - \mathsf{M}n]\rangle, \qquad (1)$$

where we denote $\tilde{h}[n] = h[-n]$. The upsampling and filtering operation results in

$$p[n] = \sum_{k\in\mathbb{Z}^d} c[k]g[n - \mathsf{M}k]. \qquad (2)$$

Writing signals as column vectors, for example $\boldsymbol{x} = (x[n] : n \in \mathbb{Z}^d)^T$, we can express these operations as matrix multiplications

$$\boldsymbol{c} = \mathsf{H}\boldsymbol{x} \quad \text{and} \quad \boldsymbol{p} = \mathsf{G}\boldsymbol{c},$$

where H and G correspond to $(\downarrow \mathsf{M})H$ and $G(\uparrow \mathsf{M})$, respectively. For example, in the usual case $d = 1$ and $\mathsf{M} = 2$, we have

$$\mathsf{H} = \begin{pmatrix} \ddots & & & & & & \\ \dots & h[2] & h[1] & h[0] & \dots & & \\ & & \dots & h[2] & h[1] & h[0] & \dots \\ & & & & & & \ddots \end{pmatrix}, \quad \text{and}$$

$$\mathsf{G} = \begin{pmatrix} \ddots & \vdots & & \\ & g[0] & & \\ & g[1] & \vdots & \\ & g[2] & g[0] & \\ & \vdots & g[1] & \\ & & g[2] & \\ & & \vdots & \ddots \end{pmatrix}. \qquad (3)$$

In general, H has $\left\{\tilde{h}[n - \mathsf{M}k]\right\}_{n\in\mathbb{Z}^d}$ as its rows and G has $\{g[n - \mathsf{M}k]\}_{n\in\mathbb{Z}^d}$ as its columns. Typically, those are infinite matrices but they can also be considered as finite matrices when dealing with finite length signals with appropriate boundary treatments. In the sequel, we denote I as the identity matrices with appropriate sizes depending on the context. Using this matrix notation, the difference signal of the LP can be written as

$$\boldsymbol{d} = \boldsymbol{x} - \boldsymbol{p} = \boldsymbol{x} - \mathsf{G}\mathsf{H}\boldsymbol{x} = (\mathsf{I} - \mathsf{G}\mathsf{H})\boldsymbol{x}.$$

By combining the previous relations, we can write the analysis operator of the LP as follows

$$\underbrace{\begin{pmatrix} \boldsymbol{c} \\ \boldsymbol{d} \end{pmatrix}}_{\boldsymbol{y}} = \underbrace{\begin{pmatrix} \mathsf{H} \\ \mathsf{I} - \mathsf{G}\mathsf{H} \end{pmatrix}}_{\mathsf{A}} \boldsymbol{x}. \qquad (4)$$

The usual inverse transform of the LP (refer to Figure 1(b)) computes: $\hat{\boldsymbol{x}} = \mathsf{G}\boldsymbol{c} + \boldsymbol{d}$, thus it can be written as

$$\hat{\boldsymbol{x}} = \underbrace{\begin{pmatrix} \mathsf{G} & \mathsf{I} \end{pmatrix}}_{\mathsf{S}_1} \begin{pmatrix} \boldsymbol{c} \\ \boldsymbol{d} \end{pmatrix}. \qquad (5)$$

It is easy to check that $\mathsf{S}_1\mathsf{A} = \mathsf{I}$ for any H and G, which agrees with the fact that the LP can be perfectly reconstructed with any pair of filters H and G.

C. Polyphase-Domain Analysis

The matrix notation for the LP operations in the previous section is simple to use but it does not reveal the matrix block structure of the LP operators as can be seen in (3). To overcome this, we introduce the *polyphase-domain* representation [10], [11] for the LP. The polyphase decomposition of a signal with respect to the sampling matrix M is a set of $|\mathsf{M}|$ sub-signals which have the same indexes modulo M, for example,

$$x_i[n] = x[\mathsf{M}n + k_i], \quad i = 0, 1, \dots, |\mathsf{M}| - 1, \qquad (6)$$

where $\{k_i\}_{0\le i<|\mathsf{M}|}$ is the set of integer vectors of the form $\mathsf{M}\boldsymbol{t}$, such that $\boldsymbol{t} \in [0, 1)^d$. The signal is reconstructed from its polyphase components by simply adding up the upsampled and shifted signals from those polyphase components. More precisely, we can write x in the z-domain as

$$X(z) = \sum_{i=0}^{|\mathsf{M}|-1} z^{-k_i} X_i(z^{\mathsf{M}}). \qquad (7)$$

Therefore, a signal can be represented by the vector of its polyphase components, that is $\boldsymbol{x}(z) \stackrel{\text{def}}{=} (X_0(z), \dots, X_{|\mathsf{M}|-1}(z))^T$. The synthesis filter G is decomposed just as the signal, while the analysis filter H has reverse phase. With this representation, the output of the filtering and downsampling operation (1) can be written as

$$c[n] = \sum_{i=0}^{|\mathsf{M}|-1} \sum_{m\in\mathbb{Z}^d} x_i[m] h_i[n - m],$$

or in the z-domain,

$$C(z) = \sum_{i=0}^{|\mathsf{M}|-1} H_i(z) X_i(z) = \mathsf{H}(z)\boldsymbol{x}(z), \qquad (8)$$

where $\mathsf{H}(z) \stackrel{\text{def}}{=} (H_0(z), \dots, H_{|\mathsf{M}|-1}(z))$. Similarly, the polyphase components of the upsampling and filtering operation (2) are

$$p_i[m] = \sum_{n\in\mathbb{Z}^d} c[n] g_i[m - n],$$

which is written in the z-domain as

$$P_i(z) = G_i(z) C(z) \quad \text{or} \quad \boldsymbol{p}(z) = \mathsf{G}(z) C(z), \qquad (9)$$

where $\mathsf{G}(z) \stackrel{\text{def}}{=} (G_0(z), \dots, G_{|\mathsf{M}|-1}(z))^T$. Therefore, the polyphase vector of the difference signal in the LP is

$$\boldsymbol{d}(z) = \boldsymbol{x}(z) - \boldsymbol{p}(z) = (\mathsf{I} - \mathsf{G}(z)\mathsf{H}(z))\, \boldsymbol{x}(z).$$

Combine these, we obtain the analysis operator of the LP in the polyphase-domain as

$$\underbrace{\begin{pmatrix} C(z) \\ \boldsymbol{d}(z) \end{pmatrix}}_{\boldsymbol{y}(z)} = \underbrace{\begin{pmatrix} \mathsf{H}(z) \\ \mathsf{I} - \mathsf{G}(z)\mathsf{H}(z) \end{pmatrix}}_{\mathsf{A}(z)} \boldsymbol{x}(z). \qquad (10)$$

This clearly resembles the time-domain representation of the LP analysis operation in (4). Therefore, in the sequel we can use the time-domain and the polyphase-domain representations interchangeably. Expressions derived for the time-domain representation also hold for the polyphase-domain representations with the obvious modifications and vice versa. Note that $\mathsf{A}(z)$ is a polynomial matrix of size $(|\mathsf{M}| + 1) \times |\mathsf{M}|$.

From this, it is straightforward that the usual inverse operator for the LP has the polyphase representation as

$$\hat{\boldsymbol{x}}(z) = \mathsf{S}_1(z)\, \boldsymbol{y}(z), \quad \text{where} \quad \mathsf{S}_1(z) = \begin{pmatrix} \mathsf{G}(z) & \mathsf{I} \end{pmatrix}.$$

D. Frame Analysis

The frame theory was originally developed by Duffin and Schaeffer [12] as a generalization of bases; for a detailed introduction, see [13], [14], [15], [16]. A family of functions

$\{\phi_k\}_{k\in\Gamma}$ in a Hilbert space H is called a *frame* if there exist two constants $\alpha > 0$ and $\beta < \infty$ such that

$$\alpha\|f\|^2 \leq \sum_{k\in\Gamma}|\langle f, \phi_k\rangle|^2 \leq \beta\|f\|^2, \quad \forall f \in H, \tag{11}$$

where α and β are called the frame bounds. When $\alpha = \beta$, the frame is said to be *tight*. Associated with a frame is the *frame operator* F, defined as the linear operator from H to $l_2(\Gamma)$ as

$$(Ff)_k = \langle f, \phi_k\rangle, \quad \text{for } k \in \Gamma. \tag{12}$$

It can be shown that the frame condition (11) is satisfied if and only if F is invertible on its range with a bounded inverse [16]. For the Laplacian pyramid, there always exists a bounded reconstruction inverse, which is the usual reconstruction, thus we immediately get the following result.

Proposition 1: The LP with stable filters[1] provides a frame expansion in $l_2(\mathbb{Z}^d)$.

As shown above, the frame operator for the LP is represented by a left matrix multiplication with A. Since the LP is a redundant transform, its frame operator admits an infinite number of left inverses. Among those, the most important is the *dual* frame operator or the *pseudo inverse* of A [17]

$$\mathsf{A}^\dagger = (\mathsf{A}^T\mathsf{A})^{-1}\mathsf{A}^T. \tag{13}$$

In the polyphase-domain, the pseudo inverse of $\mathsf{A}(z)$ is given by [18]

$$\mathsf{A}^\dagger(z) = (\mathsf{A}^*(z)\mathsf{A}(z))^{-1}\mathsf{A}^*(z). \tag{14}$$

When there is additive noise in the frame coefficients, the pseudo inverse eliminates the influence of errors that are orthogonal to the range of the frame operator. Therefore, if we have access to $\hat{\boldsymbol{y}} = \boldsymbol{y} + \boldsymbol{\eta}$ instead of $\boldsymbol{y} = \mathsf{A}\boldsymbol{x}$, then the pseudo inverse provides the solution $\hat{\boldsymbol{x}} = \mathsf{A}^\dagger\hat{\boldsymbol{y}}$ that minimizes the residual $\|\mathsf{A}\hat{\boldsymbol{x}} - \hat{\boldsymbol{y}}\|$. This is called the least-squares solution. For a tight frame, the pseudo inverse is simply the scaled transposed matrix of the frame operator, since $\mathsf{A}^T\mathsf{A} = \alpha \cdot \mathsf{I}$.

We will now review results that allow us to quantify the performance of a left inverse. It can be shown [16] that the pseudo inverse has minimum *sup norm* among all the left inverses of the frame operator. Let S be an arbitrary left inverse of A. The sup norm of an operator S is defined as

$$\|\mathsf{S}\| = \sup_{\boldsymbol{y}\neq\boldsymbol{0}} \frac{\|\mathsf{S}\boldsymbol{y}\|}{\|\boldsymbol{y}\|}, \tag{15}$$

and for a matrix, it can be computed by [17]

$$\|\mathsf{S}\| = \max\{\sqrt{\lambda} : \lambda \text{ is an eigenvalue of } \mathsf{S}\mathsf{S}^T\}. \tag{16}$$

The influence of the sup norm in the reconstruction can be seen in the following. With the noise model setup as above, the reconstruction error by S is

$$\boldsymbol{\epsilon} \stackrel{\text{def}}{=} \hat{\boldsymbol{x}} - \boldsymbol{x} = \mathsf{S}(\boldsymbol{y} + \boldsymbol{\eta}) - \boldsymbol{x} = \mathsf{S}(\mathsf{A}\boldsymbol{x} + \boldsymbol{\eta}) - \boldsymbol{x} = \mathsf{S}\boldsymbol{\eta}. \tag{17}$$

Therefore,

$$\|\boldsymbol{\epsilon}\| \leq \|\mathsf{S}\|\|\boldsymbol{\eta}\|. \tag{18}$$

[1] Stability of a filter means that a bounded input produces a bounded output.

In other words, when the energy of the noise $\boldsymbol{\eta}$ is bounded, the sup norm of the inverse matrix provides an upper bound for the reconstruction error, and this bound is tight.

In some cases, we can assume that the additive noise $\boldsymbol{\eta}$ is white and zero-mean, which means that

$$E\{\eta[i]\} = 0, \quad \text{and} \quad E\{\eta[i], \eta[j]\} = \delta[i-j]\sigma^2, \quad \text{for all } i, j, \tag{19}$$

or its autocorrelation matrix $\mathsf{R}_{\boldsymbol{\eta}} \stackrel{\text{def}}{=} E\{\boldsymbol{\eta}\boldsymbol{\eta}^T\} = \sigma^2 \cdot \mathsf{I}$. This noise model is approximately true when, for instance, $\boldsymbol{y}$ is uniformly scalar quantized. In this case, the autocorrelation of the reconstruction error by S is

$$\mathsf{R}_{\boldsymbol{\epsilon}} \stackrel{\text{def}}{=} E\{\boldsymbol{\epsilon}\boldsymbol{\epsilon}^T\} = E\{\mathsf{S}\boldsymbol{\eta}\boldsymbol{\eta}^T\mathsf{S}^T\} = \mathsf{S}\mathsf{R}_{\boldsymbol{\eta}}\mathsf{S}^T = \sigma^2\mathsf{S}\mathsf{S}^T.$$

Hence, for signals of finite length N, the reconstruction mean squared error (MSE) is [19]

$$MSE \stackrel{\text{def}}{=} \frac{E\{\|\boldsymbol{\epsilon}\|^2\}}{N} = \frac{\mathrm{tr}(\mathsf{R}_{\boldsymbol{\epsilon}})}{N} = \frac{\sigma^2\mathrm{tr}(\mathsf{S}\mathsf{S}^T)}{N} \tag{20}$$

For infinite length signals that have polyphase representation defined as before, the reconstruction MSE can be computed in the Fourier domain using the power spectrum of $\boldsymbol{\epsilon}$, which is given by [10]

$$\mathsf{R}_{\boldsymbol{\epsilon}}(e^{j\omega}) = \mathsf{S}(e^{j\omega})\mathsf{R}_{\boldsymbol{\eta}}(e^{j\omega})\mathsf{S}^*(e^{j\omega}).$$

Therefore, similarly to (20), with the white noise model given in (19) we have

$$MSE = \frac{\sigma^2}{|\mathsf{M}|(2\pi)^d}\int_{[-\pi,\pi]^d} \mathrm{tr}(\mathsf{S}(e^{j\omega})\mathsf{S}^*(e^{j\omega}))d\omega. \tag{21}$$

Since the trace of a matrix equals to the sum of its eigenvalues, the eigenvalues of $\mathsf{S}\mathsf{S}^T$ and $\mathsf{S}(e^{j\omega})\mathsf{S}^*(e^{j\omega})$ (which are also the squares of the singular values of S and $\mathsf{S}(e^{j\omega})$, respectively) play an important role in analyzing the reconstruction error due to S. Using the orthogonal projection property of the pseudo inverse, it can be shown [14], [20] that among all left inverses, the pseudo inverse minimizes the reconstruction MSE due to white noise in the frame coefficients. In summary, the pseudo inverse provides the optimal linear reconstruction.

Example 1: To get a gist of the aforementioned properties of frames, consider the following illustrative example. Consider a redundant transform that takes a scalar $x \in \mathbb{R}$ and outputs a vector $\boldsymbol{y} = (y_1, y_2)^T \in \mathbb{R}^2$ such that $y_i = x$, $i = 1, 2$. There are infinite ways to reconstruct x from $\boldsymbol{y}$: one simple way is to assign $\hat{x}_1 = y_1$, and another way is to compute $\hat{x}_2 = (y_1 + y_2)/2$. Under the white noise model given in (19), the performance by these two reconstruction methods can be quantified as: $MSE_1 = E\{\|x - \hat{x}_1\|^2\} = E\{\eta_1^2\} = \sigma^2$, and $MSE_2 = E\{\|x - \hat{x}_2\|^2\} = \frac{1}{4}E\{(\eta_1 + \eta_2)^2\} = \sigma^2/2$. Thus, we reduce the MSE by half by using the second reconstruction method instead of the first one. In fact, the second reconstruction method is the pseudo inverse, which minimizes the MSE in this case.

III. Laplacian Pyramid with Orthogonal Filters

A. The Tight Frame Case

Consider a special case where the filters in the LP are orthogonal filters with respect to the sampling matrix M, which means

$$\begin{aligned} \langle g, g[\cdot - \mathsf{M}n] \rangle &= \delta[n], \quad \text{and} & (22)\\ h[n] &= g[-n], & (23) \end{aligned}$$

or equivalently, $\mathsf{G}^T\mathsf{G} = \mathsf{I}$ and $\mathsf{H} = \mathsf{G}^T$. The condition (23) can be written in the polyphase-domain as $\mathsf{H}^*(z) = \mathsf{G}(z)$. Since

$$\langle g, g[\cdot - \mathsf{M}n] \rangle = \sum_{i=0}^{|\mathsf{M}|-1} \sum_{m \in \mathbb{Z}^d} g_i[m] g_i[m-n],$$

taking the z-transform of both sides of (22), the orthogonality condition on the filter G is equivalent to

$$\sum_{i=0}^{|\mathsf{M}|-1} G_i(z) G_i(z^{-1}) = 1 \quad \text{or} \quad \mathsf{G}^*(z)\mathsf{G}(z) = 1. \qquad (24)$$

Orthogonal filters can be designed by using well-known methods, such as separable filters from 1-D orthogonal filters [10], [11] or non-separable filters in 2-D for $\mathsf{M} = 2 \cdot \mathsf{I}_2$ [21], [22].

Theorem 1: The Laplacian pyramid with orthogonal filters is a *tight frame* with frame bounds equal to 1. Conversely, suppose the LP is a tight frame, then the frame bounds must be 1 and either $H(z) = 0$ or $\mathsf{G}(z) = \alpha(z)\mathsf{H}^*(z)$, $\mathsf{G}^*(z)\mathsf{G}(z) = \alpha(z) + \alpha(z^{-1}) - 1$.

Proof: See Appendix A ■

Remark 1: Under the orthogonality conditions, a geometrical interpretation of the tight frame can be seen by rewriting (2) as

$$p[n] = \sum_{k \in \mathbb{Z}^d} \langle x, g[\cdot - \mathsf{M}k] \rangle g[n - \mathsf{M}k].$$

Denote V the subspace spanned by the set of orthogonal vectors $\{g[\cdot - \mathsf{M}k]\}_{k \in \mathbb{Z}^d}$. Then $\boldsymbol{p}$ is the orthogonal projection of $\boldsymbol{x}$ onto V. Combine with $\boldsymbol{d} = \boldsymbol{x} - \boldsymbol{p}$, the *Pythagorean* theorem leads to

$$\|\boldsymbol{x}\|^2 = \|\boldsymbol{p}\|^2 + \|\boldsymbol{d}\|^2 = \|\boldsymbol{c}\|^2 + \|\boldsymbol{d}\|^2. \qquad (25)$$

where $\|\boldsymbol{p}\| = \|\boldsymbol{c}\|$ since $\boldsymbol{c}$ are the coefficients in the orthonormal expansion (2) of $\boldsymbol{p}$ in V. Equation (25) says that the LP is a tight frame with the frame bounds $\alpha = \beta = 1$.

Consequently, with orthogonal filters, the pseudo inverse of A is simply its transpose matrix. Thus,

$$\mathsf{A}^\dagger = \mathsf{A}^T = \begin{pmatrix} \mathsf{H} \\ \mathsf{I} - \mathsf{G}\mathsf{G}^T \end{pmatrix}^T = \begin{pmatrix} \mathsf{G} & \mathsf{I} - \mathsf{G}\mathsf{G}^T \end{pmatrix}.$$

Therefore, the reconstruction using the pseudo inverse is

$$\hat{\boldsymbol{x}} = \mathsf{A}^\dagger \boldsymbol{y} = \mathsf{G}\boldsymbol{c} + (\mathsf{I} - \mathsf{G}\mathsf{G}^T)\boldsymbol{d} = \mathsf{G}(\boldsymbol{c} - \mathsf{H}\boldsymbol{d}) + \boldsymbol{d}. \qquad (26)$$

The last expression is derived in order to reduce the computational complexity of the pseudo inverse. It leads to an efficient filter bank structure for reconstruction of the LP that is shown in Figure 3. In the polyphase domain, the pseudo inverse becomes

$$\mathsf{A}^\dagger(z) = \mathsf{A}^*(z) = \begin{pmatrix} \mathsf{G}(z) & \mathsf{I} - \mathsf{G}(z)\mathsf{G}^*(z) \end{pmatrix}.$$

We emphasize two important facts here. Firstly, the usual inverse is different from the pseudo inverse, and thus is suboptimal. We will make a precise comparison latter. Secondly, the pseudo inverse in this case has a symmetrical structure with the forward transform, and thus has the same order of complexity.

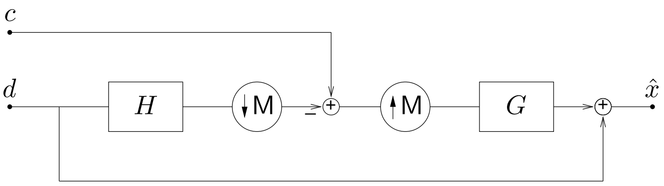

Fig. 3. The proposed reconstruction scheme for the Laplacian pyramid in Figure 1(a). It is the pseudo inverse when the filters are orthogonal.

Example 2 (The Haar case): Consider the 1-D LP with Haar filters: $\tilde{h} = g = \left(1/\sqrt{2}, 1/\sqrt{2}\right)$ and $\mathsf{M} = 2$. The output of the LP can be written as

$$\begin{aligned} c[n] &= \tfrac{1}{\sqrt{2}}x[2n] + \tfrac{1}{\sqrt{2}}x[2n+1], \\ d[2n] &= \tfrac{1}{2}x[2n] - \tfrac{1}{2}x[2n+1], \\ d[2n+1] &= -\tfrac{1}{2}x[2n] + \tfrac{1}{2}x[2n+1]. \end{aligned} \qquad (27)$$

In order to see the block structure of the transform matrices, we slightly change the notation and write $\boldsymbol{y} = (\ldots, c[n], d[2n], d[2n+1], \ldots)^T$. Using (27), the analysis matrix of the LP is a block diagonal matrix

$$\mathsf{A} = \begin{pmatrix} \ddots & & & \\ & \mathsf{B}_\mathsf{A} & & \\ & & \mathsf{B}_\mathsf{A} & \\ & & & \ddots \end{pmatrix}, \text{ where } \mathsf{B}_\mathsf{A} = \begin{pmatrix} 1/\sqrt{2} & 1/\sqrt{2} \\ 1/2 & -1/2 \\ -1/2 & 1/2 \end{pmatrix}.$$

Similarly, the usual synthesis matrix S_1 is also a block diagonal matrix with

$$\mathsf{B}_{\mathsf{S}_1} = \begin{pmatrix} 1/\sqrt{2} & 1 & 0 \\ 1/\sqrt{2} & 0 & 1 \end{pmatrix}. \qquad (28)$$

The pseudo inverse $\mathsf{A}^\dagger = \mathsf{A}^T$ is also a block diagonal matrix with $\mathsf{B}_{\mathsf{A}^\dagger} = \mathsf{B}_\mathsf{A}^T$. Since there is no overlapping between blocks, we can consider the transform for a single block with 2 inputs and 3 outputs. The eigenvalues of $\mathsf{B}_{\mathsf{A}^\dagger}\mathsf{B}_{\mathsf{A}^\dagger}^T$ are $\{1, 1\}$, while the eigenvalues of $\mathsf{B}_{\mathsf{S}_1}\mathsf{B}_{\mathsf{S}_1}^T$ are $\{1, 2\}$. Consequently,

$$\begin{aligned} &\|\mathsf{B}_{\mathsf{A}^\dagger}\| = 1, \quad \operatorname{tr}(\mathsf{B}_{\mathsf{A}^\dagger}\mathsf{B}_{\mathsf{A}^\dagger}^T) = 2, \quad \text{and} \\ &\|\mathsf{B}_{\mathsf{S}_1}\| = \sqrt{2}, \quad \operatorname{tr}(\mathsf{B}_{\mathsf{S}_1}\mathsf{B}_{\mathsf{S}_1}^T) = 3. \end{aligned}$$

Therefore, in this case if we use the pseudo inverse instead of the usual inverse, then we would reduce the upper bound of the reconstruction square error in (18) by half, and the reconstruction MSE in (20) by two-thirds.

B. Eigenvalues of the LP Operators

The improvements of the pseudo inverse over the usual inverse in the last example can be generalized for all LP's with orthogonal filters. The key is to study the eigenvalues of certain matrices. We need the following result on the eigenvalues.

Theorem 2 ([17] (p. 53)): Suppose A and B are real matrices of size $m \times n$ and $n \times m$ respectively, with $m \leq n$. Then BA has the same eigenvalues as AB, counting multiplicity, together with additional $n - m$ eigenvalues equal to 0.

For a square matrix A, denote the set of all its eigenvalues by $\sigma(\mathsf{M})$, where an eigenvalue λ with multiplicity n is written as $\lambda^{(n)}$. These eigenvalues are the roots of the characteristic polynomial of A which is defined as $P_{\mathsf{A}}(\lambda) \stackrel{\text{def}}{=} \det(\lambda \mathsf{I} - \mathsf{A})$. For a polynomial matrix $\mathsf{A}(z)$, its characteristic polynomial would generally have coefficients as polynomials of z as well. Theorem 2 says that $P_{\mathsf{BA}}(\lambda) = \lambda^{n-m} P_{\mathsf{AB}}(\lambda)$. It can be verified that this result also holds when A and B are polynomial matrices.

Proposition 2: Suppose the LP uses orthogonal filters. Then:

(a) $\sigma(\mathsf{A}^*(z)\mathsf{A}(z)) = \{1^{(|\mathsf{M}|)}\}$, and
(b) $\sigma(\mathsf{S}_1(z)\mathsf{S}_1^*(z)) = \{1^{(|\mathsf{M}|-1)}, 2\}$.

Proof: Since $\mathsf{A}(z)$ represents a tight frame with frame bounds equal to 1, we have $\mathsf{A}^*(z)\mathsf{A}(z) = \mathsf{I}$. Therefore, (a) follows directly. Next, consider $\mathsf{S}_1(z)\mathsf{S}_1^*(z) = \mathsf{G}(z)\mathsf{G}^*(z) + \mathsf{I}$. Since $\mathsf{G}^*(z)\mathsf{G}(z) = 1$ by the orthogonal condition, from Theorem 2 it follows that $\sigma(\mathsf{G}(z)\mathsf{G}^*(z)) = \{0^{(|\mathsf{M}|-1)}, 1\}$, or $P_{\mathsf{G}(z)\mathsf{G}^*(z)}(\lambda) = (\lambda - 1)\lambda^{|\mathsf{M}|-1}$. Thus,

$$\begin{aligned} P_{\mathsf{G}(z)\mathsf{G}^*(z)+\mathsf{I}}(\lambda) &= \det(\lambda \mathsf{I} - \mathsf{G}(z)\mathsf{G}^*(z) - \mathsf{I}) \\ &= P_{\mathsf{G}(z)\mathsf{G}^*(z)}(\lambda - 1) \\ &= (\lambda - 2)(\lambda - 1)^{|\mathsf{M}|-1}, \end{aligned}$$

which implies (b). ∎

Recall that with orthogonal filters, the pseudo inverse of the LP is $\mathsf{A}^\dagger(z) = \mathsf{A}^*(z)$. Thus, from (16) and (21) we immediately obtain the following results.

Corollary 1: Suppose the LP uses orthogonal filters. Then:

(a) $\|\mathsf{S}_1\| = \sqrt{2}$, and
(b) $\|\mathsf{A}^\dagger\| = 1$.

As a result, when the noise energy is bounded, the upper bound of the reconstruction square error in (18) using the pseudo inverse is equal to half of the one that uses the usual inverse.

Corollary 2: Suppose the LP uses orthogonal filters and its coefficients are contaminated by an additive white noise with variance σ^2. Then for *one level* LP the reconstruction mean square error using the usual inverse is $MSE_1 = \sigma^2(1 + 1/|\mathsf{M}|)$, while using the pseudo inverse it is $MSE_2 = \sigma^2$. When the LP *is iterated with J-levels*, then for the usual inverse we have

$$MSE_1^{(J)} = \sigma^2 \left(1 + \frac{1}{|\mathsf{M}|} + \ldots + \frac{1}{|\mathsf{M}|^J}\right) \to \sigma^2 \frac{|\mathsf{M}|}{|\mathsf{M}| - 1},$$

while for the pseudo inverse we still have $MSE_2^{(J)} = \sigma^2$.

Therefore, with white noise on the LP coefficients, the reduction in the reconstruction MSE by using the pseudo inverse instead of using the usual inverse is from $(1 + 1/|\mathsf{M}|)$ times for one level LP up to $(1 + 1/(|\mathsf{M}| - 1))$ times for multiple levels LP's. In particular, for the commonly used LP in 2-D with $\mathsf{M} = 2 \cdot \mathsf{I}_2$, the pseudo inverse improves the signal-to-noise ratio (SNR) of the reconstruction signal from 0.97 dB (with one level LP) up to 1.25 dB (with iterated LP).

Remark 2: Let us clarify the difference in the performance measurements between Corollary 1 and Corollary 2. The results in Corollary 1 use the *maximal* eigenvalues from Proposition 2, whereas the results in Corollary 2 use the *average* of these eigenvalues. Thus, the gain factor by the pseudo inverse in Corollary 1 is fixed, while the gain factor in Corollary 2 gets smaller as $|\mathsf{M}|$ becomes larger.

Finally, we have the following properties on the operators that reconstruct from the coarse and difference signals using the pseudo inverse.

Proposition 3: Consider $\mathsf{G}(z)$ and $\mathsf{D}(z) = \mathsf{I} - \mathsf{G}(z)\mathsf{H}(z)$. Suppose the LP uses orthogonal filters. Then:

(a) $\sigma(\mathsf{G}(z)\mathsf{G}^*(z)) = \{0^{(|\mathsf{M}|-1)}, 1\}$,
(c) $\mathsf{D}^*(z) = \mathsf{D}(z)$,
(b) $\mathsf{D}(z)\mathsf{D}(z) = \mathsf{D}(z)$,
(d) $\sigma(\mathsf{D}(z)) = \{0, 1^{(|\mathsf{M}|-1)}\}$.

Proof: Part (a) was proved in the proof of Proposition 2. Part (b) and (c) are easily verified using the orthogonal conditions: $\mathsf{G}^*(z)\mathsf{G}(z) = 1$ and $\mathsf{H}(z) = \mathsf{G}^*(z)$. Using characteristic polynomials similarly to the proof of Proposition 2, part (d) is proved by observing that $P_{\mathsf{D}(z)}(\lambda) = \pm P_{\mathsf{G}(z)\mathsf{G}^*(z)}(1 - \lambda)$. ∎

As a result, the operator for the difference signal in the LP, $\boldsymbol{d} = (\mathsf{I} - \mathsf{GH})\boldsymbol{x}$, is an orthogonal projection to a subspace, which has dimension equal to $(|\mathsf{M}| - 1)/|\mathsf{M}|$ times the dimension of the signal space.[2] Such a view can also be inferred from the geometrical proof of Theorem 1.

IV. Reconstruction using Projection

A. The New Reconstruction Algorithm

In this section, we consider a more general case when H and G are arbitrary filters. Even though any frame operator has a pseudo inverse, for complexity reason, we will consider only the inverses that can be realized by a structured transform with fast algorithm. Motivated by the tight frame case, we focus on the reconstruction that has a structure shown in Figure 3. We then turn the problem around by asking for which filters such an algorithm is indeed an inverse or pseudo inverse. This has the same flavor as the filter design problem for perfect reconstruction filter banks, thus we can resort to many existing results.

Theorem 3:

1) The reconstruction shown in Figure 3 is an inverse transform of the LP *if and only if* two filters H and G are biorthogonal with respect to the sampling lattice M, which means the prediction operator of the LP (GH) is a projector, or $\mathsf{HG} = \mathsf{I}$.

[2] For infinite length signals, this has to be interpreted in the polyphase-domain.

2) Furthermore, that reconstruction is the pseudo inverse *if and only if* the prediction operator of the LP (GH) is an orthogonal projector.[3]

Proof: See Appendix B ■

Remark 3: It is interesting to note that the two conditions for the LP in the above proposition, i.e. projection and orthogonal projection, are exactly the same as the conditions for the improved LP's that are studied in [23]. Those conditions lead to LP with interpolation and least squares LP, respectively. The motivation for those modifications there is to minimize the prediction error $\boldsymbol{d}$ of the LP, whereas our motivation is to have a better reconstruction algorithm for the LP. Still, the results from [23] motivate the use of filters with the aforementioned properties for the LP.

Remark 4: The orthogonal projection case obviously includes the LP with orthogonal filters studied in the last section. It is shown in [23] that under the orthogonal projection condition, if one of the LP filter is given, then the other filter is uniquely determined.

Therefore, the minimum requirement for the FB shown in Figure 3 to be a bona fide inverse of the LP is the biorthogonality condition (56) on the filters H and G, which can be expressed equivalently in the polyphase-domain as $\mathsf{H}(z)\mathsf{G}(z) = 1$. There exist many designs for such filters due to their role in wavelet constructions [24], [25]. Among them, a popular choice for images is the "9-7" filters from [24], [25]. Another example is based on the original LP filter suggested in [1], which is especially popular for applications in vision, together with its dual filter [26]. Tables I and II list these filter coefficients. Note that these filters are symmetric and close to being orthogonal. As a result, the proposed reconstruction in Figure 3 is close to the pseudo inverse.

With biorthogonal filters, the proposed reconstruction algorithm for the LP has an intuitive geometrical interpretation. Let us define two subspaces V and $\tilde{V}$ that are spanned by $\{g[\cdot - \mathsf{M}k]\}_{k \in \mathbb{Z}^d}$ and $\{\tilde{h}[\cdot - \mathsf{M}k]\}_{k \in \mathbb{Z}^d}$, respectively. These are also the column and row spaces of G and H, respectively. For all $\boldsymbol{x}$ in $l_2(\mathbb{Z}^d)$, the prediction operator in the LP, $\boldsymbol{p} = \mathsf{GH}\boldsymbol{x}$, computes a projection of $\boldsymbol{x}$ onto V. Since $\mathsf{HG} = \mathsf{I}$, the difference signal $\boldsymbol{d} = \boldsymbol{x} - \boldsymbol{p}$ has the property that

$$\mathsf{H}\boldsymbol{d} = \mathsf{H}(\boldsymbol{x} - \mathsf{GH}\boldsymbol{x}) = \mathsf{H}\boldsymbol{x} - \mathsf{H}\boldsymbol{x} = \boldsymbol{0}.$$

Therefore, $\boldsymbol{d}$ is perpendicular to $\tilde{V}$. This fact is illustrated in Figure 4(a). The prediction operator in the LP (GH) can be called an *oblique projector* [27] and denoted by P_V.

Let us define W the orthogonal complementary subspace of $\tilde{V}$. Then it is easy to verify that $\boldsymbol{d} = \boldsymbol{x} - P_V\boldsymbol{x}$ is a projection of $\boldsymbol{x}$ onto W such that the error is parallel to V (again, refer to Figure 4(a)). Denote this projection as P_W, $P_W = \mathsf{I} - \mathsf{GH}$.

Next, let us compare the usual reconstruction method as in Figure 1(b), denoted REC-1,

$$\hat{\boldsymbol{x}}_1 = \mathsf{S}_1\boldsymbol{y} = \mathsf{G}\boldsymbol{c} + \boldsymbol{d}, \tag{29}$$

with the new reconstruction using the FB as in Figure 3, denoted REC-2,

$$\hat{\boldsymbol{x}}_2 = \mathsf{S}_2\boldsymbol{y} = \mathsf{G}\boldsymbol{c} + (\mathsf{I} - \mathsf{GH})\boldsymbol{d}. \tag{30}$$

These two reconstruction algorithms are different in the way of handling the difference signal $\boldsymbol{d}$. More specifically, the REC-1 method adds $\boldsymbol{d}$ directly while the REC-2 method adds the P_W projection of $\boldsymbol{d}$ to the reconstructed signal. As shown in Figure 4(b), when there is noise in the LP coefficients, the REC-2 method eliminates the influence of the error component in $\hat{\boldsymbol{d}}$ that is parallel to V.

For more quantitative measurements on the performance of the two methods, suppose that we wish to approximate $\boldsymbol{x}$ given $\hat{\boldsymbol{y}} = \mathsf{A}\boldsymbol{x} + \boldsymbol{\eta}$. With no further information about the error in the LP coefficients $\boldsymbol{\eta}$, it makes sense to chose $\hat{\boldsymbol{x}}$ that minimizes the residual $\|\mathsf{A}\hat{\boldsymbol{x}} - \hat{\boldsymbol{y}}\|$. As mentioned before, the optimal linear solution to this problem is the pseudo inverse of A. Using this as the measurement for the performance in reconstruction, the following result states that REC-2 always performs better than REC-1.

Proposition 4: Assume that H and G are biorthogonal filters. Let $\hat{\boldsymbol{x}}_1$ and $\hat{\boldsymbol{x}}_2$ be the results of reconstruction from noisy LP coefficients $\hat{\boldsymbol{y}}$ using REC-1 and REC-2, respectively. Then we have

$$\|\mathsf{A}\hat{\boldsymbol{x}}_1 - \hat{\boldsymbol{y}}\| \geq \|\mathsf{A}\hat{\boldsymbol{x}}_2 - \hat{\boldsymbol{y}}\|, \tag{31}$$

where equality holds if and only if $\mathsf{H}\hat{\boldsymbol{d}} = \boldsymbol{0}$.

Proof: Using the definition of A, S_1, S_2 in (4), (5), (55) and the fact that $\mathsf{GH} = \mathsf{I}$, we have after some manipulations

$$\begin{aligned} \mathsf{A}\hat{\boldsymbol{x}}_1 - \hat{\boldsymbol{y}} &= \mathsf{AS}_1\hat{\boldsymbol{y}} - \hat{\boldsymbol{y}} = \begin{pmatrix} \mathsf{H}\hat{\boldsymbol{d}} \\ -\mathsf{GH}\hat{\boldsymbol{d}} \end{pmatrix}, \quad \text{and} \\ \mathsf{A}\hat{\boldsymbol{x}}_2 - \hat{\boldsymbol{y}} &= \mathsf{AS}_2\hat{\boldsymbol{y}} - \hat{\boldsymbol{y}} = \begin{pmatrix} \boldsymbol{0} \\ -\mathsf{GH}\hat{\boldsymbol{d}} \end{pmatrix}. \end{aligned}$$

Therefore,

$$\|\mathsf{A}\hat{\boldsymbol{x}}_1 - \hat{\boldsymbol{y}}\|^2 = ||\mathsf{H}\hat{\boldsymbol{d}}||^2 + ||\mathsf{GH}\hat{\boldsymbol{d}}||^2 \geq ||\mathsf{GH}\hat{\boldsymbol{d}}||^2 = \|\mathsf{A}\hat{\boldsymbol{x}}_2 - \hat{\boldsymbol{y}}\|^2.$$

■

B. Reconstruction Error Analysis

Note that the above comparison does not give us exact behavior of the reconstruction error. In this section, we will study this error under some additional assumptions on the coefficient noise. Our analysis is complicated further since in coding, the LP is often used with quantization noise feedback where the coarse signal c is quantized *before* being fed back to the predictor. This case is referred to as the closed-loop mode in Figure 5. The open-loop mode refers to the case that has been considered so far, namely, when the noise is added to the coefficients *after* the LP transform. A discussion of those two quantization modes in pyramid coding can be found in [28]. Note that with the closed-loop mode, we are no longer in the linear framework, so that optimality of the pseudo-inverse does not hold.[4]

[3] Recall that given a Hilbert space H, a linear operator P mapping H onto itself is called a *projector* if $P^2 = P$. Furthermore, if P is self-adjoint or $P = P^T$ then P is called an *orthogonal projector*.

[4] In that case, a *consistent reconstruction* algorithm [29] can lead to improvements.

n	0	±1	±2	±3	±4
$h[n]$	0.852699	0.377403	-0.110624	-0.023849	0.037828
$g[n]$	0.788486	0.418092	-0.040689	-0.064539	

TABLE I

COEFFICIENTS FOR THE "9-7" BIORTHOGONAL FILTERS.

n	0	±1	±2	±3
$h[n]/\sqrt{2}$	0.6	0.25	-0.05	0
$g[n]/\sqrt{2}$	0.607143	0.260714	-0.053571	-0.010714

TABLE II

COEFFICIENTS FOR THE ORIGINAL LP FILTER AND ITS DUAL FILTER.

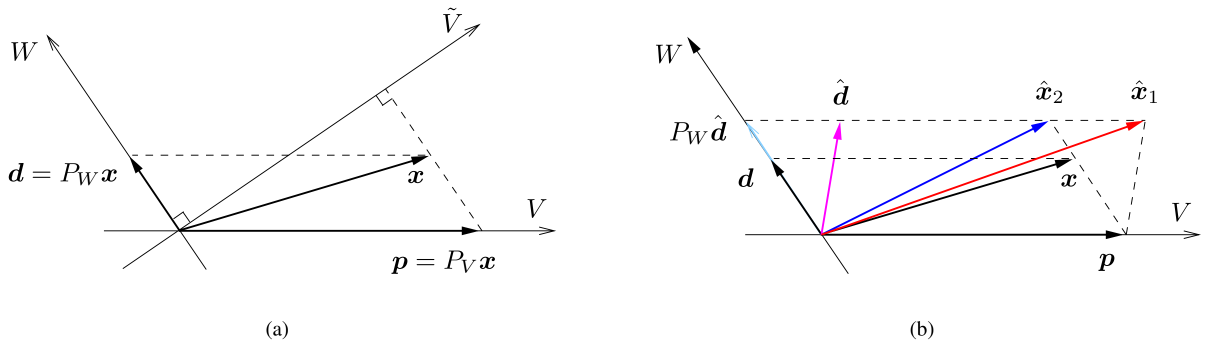

Fig. 4. Geometrical interpretation of the LP with biorthogonal filters. (a) The LP as an oblique projector: $\boldsymbol{p} = P_V \boldsymbol{x}$ is the projection of x onto V such that the difference signal $\boldsymbol{d} = \boldsymbol{x} - P_V \boldsymbol{x}$ is perpendicular to $\tilde{V}$. (b) Comparing two reconstruction methods when $\boldsymbol{d}$ is corrupted by noise and becomes $\hat{\boldsymbol{d}}$. The usual reconstruction REC-1 adds $\hat{\boldsymbol{d}}$ directly to the reconstructed signal, while the new reconstruction REC-2 adds the P_W projection of $\hat{\boldsymbol{d}}$ and thus eliminates the error component in $\hat{\boldsymbol{d}}$ that is parallel to V.

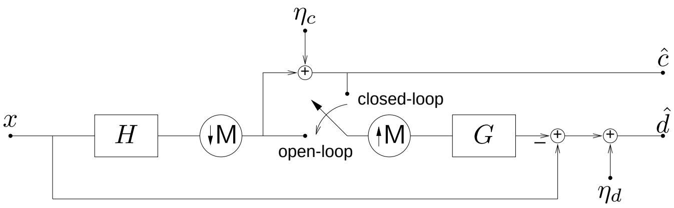

Fig. 5. Laplacian pyramid encoding. The open-loop mode bypasses the coarse level quantization, whereas the closed-loop mode includes it.

To analyze the reconstruction error, we separate the noise in the LP coefficients into two components: $\boldsymbol{\eta} = (\boldsymbol{\eta}_c, \boldsymbol{\eta}_d)^T$, corresponding to the coarse and detail quantization as shown in Figure 5. In the open-loop (ol) mode, we can apply (17) to obtain the reconstruction errors using REC-1 and REC-2 as

$$\begin{aligned} \boldsymbol{\epsilon}_1^{(\text{ol})} &= \mathsf{G}\boldsymbol{\eta}_c + \boldsymbol{\eta}_d, \quad \text{and} \\ \boldsymbol{\epsilon}_2^{(\text{ol})} &= \mathsf{G}\boldsymbol{\eta}_c + (\mathsf{I} - \mathsf{GH})\boldsymbol{\eta}_d. \end{aligned} \tag{32}$$

In the closed-loop (cl) mode, by direct computation we obtain the reconstruction errors using REC-1 and REC-2 as

$$\begin{aligned} \boldsymbol{\epsilon}_1^{(\text{cl})} &= \boldsymbol{\eta}_d, \quad \text{and} \\ \boldsymbol{\epsilon}_2^{(\text{cl})} &= \mathsf{G}\boldsymbol{\eta}_c + (\mathsf{I} - \mathsf{GH})\boldsymbol{\eta}_d. \end{aligned} \tag{33}$$

From (32) and (33) we observe that with the REC-1 method, the coarse level noise $\boldsymbol{\eta}_c$ does not effect the reconstruction signal in the closed-loop mode. This makes the usual reconstruction method REC-1 attractive in coding application. However, the problem of allocating bits to the quantizers Q_c and Q_d for the coarse and difference signals becomes difficult. The reason is that in minimizing $\boldsymbol{\epsilon}_1^{(\text{cl})}$, the choice for Q_d depends on the choice for Q_c, and thus one must use a complicated bit allocation technique [28]. On the other hand, with the new method REC-2, the reconstruction errors are the same in both open- and closed-loop modes, thus we can simply use the open-loop mode. Furthermore, when the filters are close to being orthogonal, because $\|\boldsymbol{\epsilon}\|^2 \approx \|\boldsymbol{\eta}\|^2$, the square error distortion can be minimized in the LP domain using much simpler bit allocation techniques such as [30].

Now suppose that $\|\boldsymbol{\eta}_c\|$ is negligible compared to $\|\boldsymbol{\eta}_d\|$. This is a reasonable assumption since $\boldsymbol{\eta}_c$ has $|\mathsf{M}|$ times fewer samples than $\boldsymbol{\eta}_d$. Furthermore, suppose that the predictor (GH) becomes an orthogonal projection which implies $\|(\mathsf{I} - \mathsf{GH})\boldsymbol{\eta}_d\| \leq \|\boldsymbol{\eta}_d\|$. Under these conditions in both modes, we have: $\|\boldsymbol{\epsilon}_2\| \leq \|\boldsymbol{\epsilon}_1\|$, or REC-2 performs better than REC-1. A finer analysis under the additive white noise model is provided by the following result.

Proposition 5: Suppose the LP use orthogonal filters and the additive noises $\boldsymbol{\eta}_c$ and $\boldsymbol{\eta}_d$ to the LP coefficients are uncorrelated white with variances σ_c^2 and σ_d^2, respectively. Then the reconstruction mean square errors by using REC-1 and REC-2 are:

(a) For the open-loop mode:

$$MSE_1^{(\mathrm{ol})} = \frac{1}{|\mathsf{M}|}\sigma_c^2 + \sigma_d^2$$
$$MSE_2^{(\mathrm{ol})} = \frac{1}{|\mathsf{M}|}\sigma_c^2 + \frac{|\mathsf{M}|-1}{|\mathsf{M}|}\sigma_d^2$$

(b) For the closed-loop mode:

$$MSE_1^{(\mathrm{cl})} = \sigma_d^2$$
$$MSE_2^{(\mathrm{cl})} = \frac{1}{|\mathsf{M}|}\sigma_c^2 + \frac{|\mathsf{M}|-1}{|\mathsf{M}|}\sigma_d^2$$

Proof: Since $\boldsymbol{\eta}_c$ and $\boldsymbol{\eta}_d$ are uncorrelated and white, applying (21) to (32) we have

$$MSE_2^{(\mathrm{ol})} = \frac{\sigma_c^2}{|\mathsf{M}|(2\pi)^d}\int_{[-\pi,\pi]^d} \mathrm{tr}(\mathsf{G}(e^{j\omega})\mathsf{G}^*(e^{j\omega}))d\omega + \frac{\sigma_d^2}{|\mathsf{M}|(2\pi)^d}\int_{[-\pi,\pi]^d} \mathrm{tr}(\mathsf{D}(e^{j\omega})\mathsf{D}^*(e^{j\omega}))d\omega.$$

From this, using Proposition 3 we get the desired result for $MSE_2^{(\mathrm{ol})}$. Other results follow similarly. ∎

Numerical results on real images follow the above analysis very closely, even for filters that are only approximately orthogonal such as the “9-7” biorthogonal filters in Table I (which was used in all of our experiments). For example, in the image coding application, assume that uniform scalar quantizers with equal step for coarse and difference signals, $\Delta_c = \Delta_d = \Delta$ are used, then we have $\sigma_c^2 \approx \sigma_d^2 \approx \Delta^2/12$. In this case, the new inverse REC-2 improves the SNR of the reconstructed signal over the usual inverse REC-1 by $10\log_{10}(5/4) = 0.97$ dB in the open-loop mode, while giving the same performance as the usual inverse in the closed-loop mode. Figure 6 shows the result for the “Barbara” image of size 512×512.

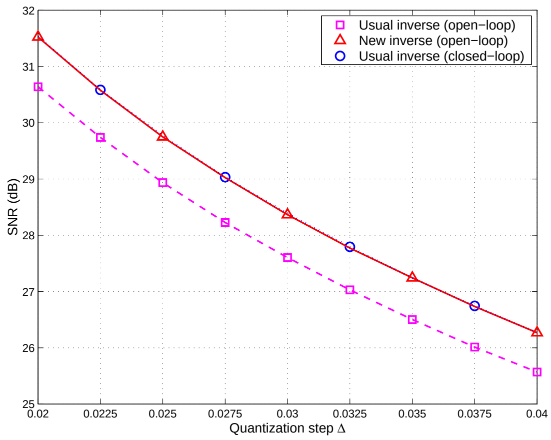

Fig. 6. Comparison of reconstructions from the quantized LP coefficients of the “Barbara” image. The LP is decomposed with just two levels.

In some other applications like denoising, the LP coefficients are thresholded so that only the M most significant coefficients are retained. (This is normally done in the open-loop mode.) In this case, it is difficult to model the coefficient noise which strongly depends on the input signal. Table III presents the numerical results for some standard test images. We observe that the new inverse consistently provides better performance by around 0.5 dB in SNR.

M		2^{12}	2^{14}	2^{16}
Barbara	REC-1	9.68	12.56	20.94
	REC-2	**9.87**	**13.18**	**21.75**
Goldhill	REC-1	12.30	15.79	21.55
	REC-2	**12.60**	**16.23**	**22.19**
Peppers	REC-1	15.06	20.81	26.77
	REC-2	**15.62**	**21.33**	**27.32**

TABLE III

SNR’S OF THE RECONSTRUCTED SIGNALS FROM THE M MOST SIGNIFICANT LP COEFFICIENTS. THE IMAGE SIZES ARE 512×512. THE LP IS DECOMPOSED WITH SIX LEVELS.

V. LAPLACIAN PYRAMID AS AN OVERSAMPLED FILTER BANK

A. Equivalent Filters in an Oversampled Filter Bank

The polyphase matrices for the LP operators given in Section II-C suggest that we can treat each polyphase component of the difference signal separately as being filtered and downsampled by M. We can reformulate the LP as an oversampled FB as shown in Figure 7. Note that every LP can be expressed as an oversampled FB, but not every oversampled filter bank in Figure 7 corresponds to a LP structure, since we will see that for the LP, all filters K_i are specified by H and G.

From (10), it follows that the polyphase vector for the equivalent filter K_i is the $(i+1)$-st row of the matrix $\mathsf{I} - \mathsf{G}(z)\mathsf{H}(z)$, which is equal to $\boldsymbol{e}_i^T - G_i(z)\mathsf{H}(z)$, where $\boldsymbol{e}_i$ is the $(i+1)$-st column of the identity matrix. Thus,

$$K_i(z) = z^{k_i} - G_i(z^{\mathsf{M}})H(z), \quad \text{for } i = 0,\ldots,|\mathsf{M}|-1. \quad (34)$$

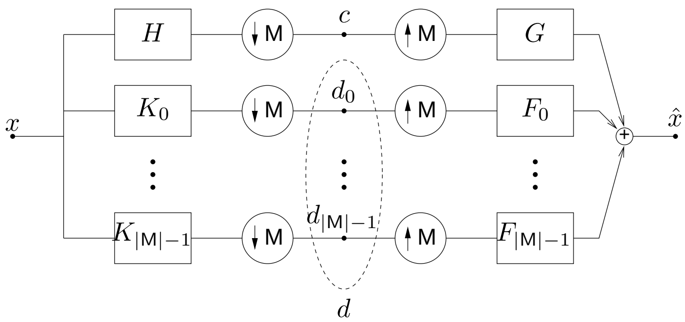

Fig. 7. Laplacian pyramid as an oversampled filter bank, where $\{d_0,\ldots,d_{|\mathsf{M}|-1}\}$ are the polyphase components of d.

Similarly, on the synthesis side, for the REC-1 method, the equivalent filter $F_i^{[1]}$ has the polyphase vector as $\boldsymbol{e}_i$, therefore

$$F_i^{[1]}(z) = z^{-k_i}, \quad \text{for } i = 0,\ldots,|\mathsf{M}|-1. \quad (35)$$

For the REC-2 method, the equivalent filters $F_i^{[2]}$ has the polyphase vector as $\boldsymbol{e}_i - \mathsf{G}(z)H_i(z)$, which implies that

$$F_i^{[2]}(z) = z^{-k_i} - G(z)H_i(z^{\mathsf{M}}), \quad \text{for } i = 0,\ldots,|\mathsf{M}|-1. \quad (36)$$

Since $H(z)$ and $G(z)$ are both lowpass filters, it is easy to see that $K_i(z)$ and $F_i^{[2]}(z)$ are highpass filters, whereas $F_i^{[1]}(z)$ are allpass filters. Figure 8 displays the frequency responses of the equivalent filters for the LP in 1-D using the biorthogonal filter pair "9-7" from Table I.

In the 1-D case with $M = 2$ and biorthogonal filters, using the property $G_0(z)H_0(z)+G_1(z)H_1(z) = 1$, we can simplify the expressions for equivalent filters in (34) as

$$\begin{aligned} K_0(z) &= -zH_1(z^2)G(-z) \\ K_1(z) &= +zH_0(z^2)G(-z), \end{aligned}$$

and for the synthesis filters of the REC-2 method as

$$\begin{aligned} F_0^{[2]}(z) &= -z^{-1}G_1(z^2)H(-z) \\ F_1^{[2]}(z) &= +z^{-1}G_0(z^2)H(-z) \end{aligned}$$

As a result, if the LP filters $H(e^{j\omega})$ and $G(e^{j\omega})$ are designed to have p_h and p_g zeros at $\omega = \pi$, then $K_i(e^{j\omega})$ and $F_i^{[2]}(e^{j\omega})$ have p_g and p_h zeros at $\omega = 0$, respectively. This result can be observed in Figure 8 for the "9-7" case where $p_h = p_g = 4$. The number of zeros at $\omega = \pi$ of the filter determines the maximum degree of polynomials that can be reproduced by that filter and is referred to the *accuracy* number [31]. The number of zeros at $\omega = 0$ indicates the maximum degree of polynomial that are annihilated by the filters and is referred to the number of *vanishing moments*. Therefore, the LP with high accuracy filters also has good compression properties for polynomial signals. For example, for the LP with "9-7" filters, the output $d[n]$ is zero whenever the input is a polynomial signal of degree up to three.

B. General Reconstruction

An interesting question is, what is the most general reconstruction for a given LP? In the polyphase-domain, this is equivalent to determine the most general form of the synthesis polyphase matrix $\mathsf{S}(z)$ such that it satisfies the following perfect reconstruction (PR) condition [10], [11]

$$\mathsf{S}(z)\mathsf{A}(z) = \mathsf{I}. \tag{37}$$

Corresponding to a polyphase matrix $\mathsf{S}(z)$ satisfying the PR condition (37) is a set of synthesis filters G and F_i for the FB in Figure 7 so the input signal can be perfectly reconstructed from the output of the LP. One parameterization for the left inverse of $\mathsf{A}(z)$ is given in [32] as

$$\mathsf{S}(z) = \tilde{\mathsf{S}}(z) + \mathsf{U}(z)[I - \mathsf{A}(z)\tilde{\mathsf{S}}(z)] \tag{38}$$

where $\tilde{\mathsf{S}}(z)$ is any particular left inverse of A, and $\mathsf{U}(z)$ is an $|\mathsf{M}| \times (|\mathsf{M}| + 1)$ matrix with bounded entries. In our case, a good choice for $\tilde{\mathsf{S}}(z)$ is the usual inverse $\mathsf{S}_1(z) = \begin{pmatrix}\mathsf{G}(z) & \mathsf{I} - \mathsf{G}(z)\mathsf{H}(z)\end{pmatrix}$. Let us split $\mathsf{S}(z)$ into two sub-matrices $\mathsf{S}_c(z)$ and $\mathsf{S}_d(z)$ of size $|\mathsf{M}| \times 1$ and $|\mathsf{M}| \times |\mathsf{M}|$, respectively: $\mathsf{S}(z) = \begin{pmatrix}\mathsf{S}_c(z) & \mathsf{S}_d(z)\end{pmatrix}$; and similarly for $\mathsf{U}(z)$: $\mathsf{U}(z) = \begin{pmatrix}\mathsf{U}_c(z) & \mathsf{U}_d(z)\end{pmatrix}$. Then the reconstruction for the LP using such $\mathsf{S}(z)$ can be written in polyphase-domain as

$$\hat{\boldsymbol{x}}(z) = \mathsf{S}_c(z)C(z) + \mathsf{S}_d(z)\boldsymbol{d}(z)$$

Substituting $\tilde{\mathsf{S}}(z) = \mathsf{S}_1(z)$ into (38) and after some manipulations on the block matrices, we obtain the following result.

Theorem 4: The most general form for the synthesis polyphase matrix providing perfect reconstruction for a LP can be written as $\mathsf{S}(z) = \begin{pmatrix}\mathsf{S}_c(z) & \mathsf{S}_d(z)\end{pmatrix}$ with

$$\begin{aligned} \mathsf{S}_c(z) &= \mathsf{G}(z) - [\mathsf{U}_c(z) - \mathsf{U}_d(z)\mathsf{G}(z)]\,[\mathsf{H}(z)\mathsf{G}(z) - 1], \\ \mathsf{S}_d(z) &= \mathsf{I} - [\mathsf{U}_c(z) - \mathsf{U}_d(z)\mathsf{G}(z)]\,\mathsf{H}(z), \end{aligned} \tag{39}$$

and where $\mathsf{U}_c(z)$ and $\mathsf{U}_d(z)$ are matrices of size $|\mathsf{M}| \times 1$ and $|\mathsf{M}| \times |\mathsf{M}|$, respectively, with bounded entries.

As a consequence of the above result, for a given LP, matrices $\mathsf{U}_c(z)$ and $\mathsf{U}_d(z)$ can be optimized so that the resulting synthesis filters have certain desired properties. We observe that if the LP uses biorthogonal filters satisfying $\mathsf{H}(z)\mathsf{G}(z) = 1$, then from (39) we have $\mathsf{S}_c(z) = \mathsf{G}(z)$. This means that all the synthesis FB's providing perfect reconstruction for the LP in this case necessarily have G as the synthesis filter for the coarse channel.

Example 3: Let us consider the LP with Haar filters as in Example 2. In this case, we have $H_0(z) = H_1(z) = G_0(z) = G_1(z) = 1/\sqrt{2}$. By applying (39) and denoting $V_i(z) = (-2\mathsf{U}_{i,1}(z) + \mathsf{U}_{i,2}(z) + \mathsf{U}_{i,3}(z))/(2\sqrt{2}),\ i = 1, 2$, any synthesis polyphase matrices $\mathsf{S}(z)$ providing PR can be written as

$$\mathsf{S}(z) = \begin{pmatrix} G_0(z) & 1 + V_1(z) & V_1(z) \\ G_1(z) & V_2(z) & 1 + V_2(z) \end{pmatrix}.$$

Thus, by denoting $V(z) = V_1(z^2) + z^{-1}V_2(z^2)$, we obtain the most general form of synthesis filters for the Haar LP are: $G(z)$, $F_0(z) = 1 + V(z)$, and $F_1(z) = z^{-1} + V(z)$, with any stable filter $V(z)$. The usual and pseudo inverses correspond to $V(z) = 0$ and $V(z) = (-1 + z^{-1})/2$, respectively.

VI. Iterated Laplacian Pyramids and Derived Continuous Frames

A. Iterated Laplacian Pyramids

We now shift our focus to multilevel LP's where the scheme in Figure 1 is iterated on the coarse signal. The oversampled FB representation of the LP in Figure 7 allows us to analyze the multilevel LP as an iterated FB. Using the multirate identity, which says that filtering by $G(z)$ followed by upsampling by M is equivalent to upsampling by M followed by filtering by $G(z^{\mathsf{M}})$ [10], [11], we have the following equivalent synthesis filters at the n-level of a multilevel LP as

$$F_i^{(n)}(z) = F_i(z^{\mathsf{M}^{n-1}}) \prod_{j=0}^{n-2} G(z^{\mathsf{M}^j}), \quad i = 0, \ldots, |\mathsf{M}| - 1. \tag{40}$$

Next, consider what happens, when the synthesis filters in (35) and (36) are substituted into (40). Figure 9 shows an example of frequency responses for the equivalent filters. In the REC-1 method, we see that the synthesis functions for the LP are all low frequency signals. Thus, the errors from highpass subbands of a multilevel LP do not remain in these subbands but appear as broadband noise in the reconstructed signal. In [33], this effect was noted as the most serious disadvantage of the LP for coding applications.

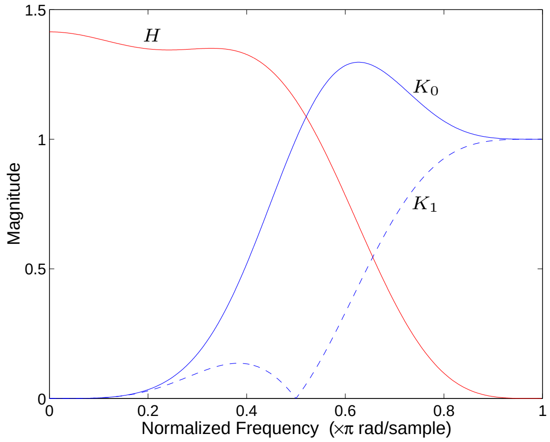

(a)

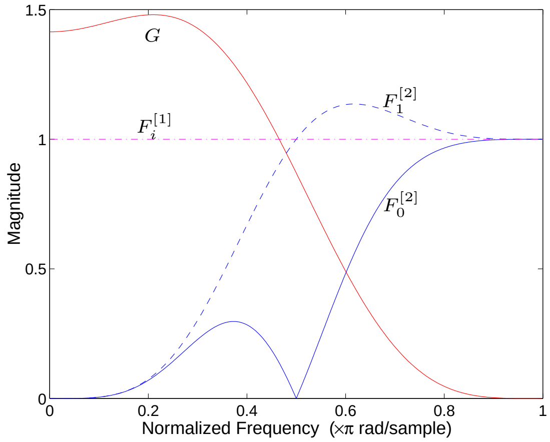

(b)

Fig. 8. Frequency responses of the equivalent filters for the LP using the biorthogonal filter pair "9-7". (a) Analysis. (b) Synthesis, using the usual (REC-1, denoted by superscript $^{[1]}$) and the new (REC-2, denoted by superscript $^{[2]}$) methods.

In the REC-2 method, the synthesis functions have similar frequency characteristics as the analysis functions, which are essentially highpass filters. Clearly, reconstruction using the REC-2 method remedies the previous mentioned problem of the LP.

The advantage of the new reconstruction method REC-2 over REC-1 is even more prominent when the errors in the LP coefficients have non-zero mean. In such case, with the REC-1 method, this non-zero mean propagates through all the lowpass synthesis filters and appears in the reconstructed signal. By contrast, with the REC-2 method, the non-zero mean is canceled by the bandpass synthesis filters. Figure 10 shows an example of this situation where the errors in the LP coefficients are uniformly distributed in $[0, 0.1]$.

B. Framelets from the Laplacian Pyramid

As iterated orthogonal filter banks lead to wavelets, a multilevel LP is associated with a frame for continuous functions that is called wavelet frame or framelets [34], [35]. We concentrate first on the orthogonal case. Using the multiresolution analysis framework by Mallat and Meyer [36], [37], [16], it follows that, under certain conditions, associated with the orthogonal lowpass filter G in the LP is an orthonormal scaling function $\phi(t) \in L^2(\mathbb{R}^d)$ that generates a multiresolution analysis (MRA) represented by a sequence of nested subspaces $\{V_j\}_{j\in\mathbb{Z}}$,

$$\dots V_2 \subset V_1 \subset V_0 \subset V_{-1} \subset V_{-2} \dots \tag{41}$$

with

$$\begin{aligned} \text{Closure}\left(\bigcup_{j\in\mathbb{Z}} V_j\right) &= L^2(\mathbb{R}^d), & (42)\\ \bigcap_{j\in\mathbb{Z}} V_j &= \{0\}. & (43)\end{aligned}$$

The scaling function ϕ is specified from the filter G via the two-scale equation:

$$\phi(t) = |\mathsf{M}|^{1/2} \sum_{n\in\mathbb{Z}^d} g[n]\phi(\mathsf{M}t - n) \tag{44}$$

Denote

$$\phi_{j,n}(t) = |\mathsf{M}|^{-j/2}\phi(\mathsf{M}^{-j}t - n), \quad j \in \mathbb{Z}, n \in \mathbb{Z}^d. \tag{45}$$

Then the family $\{\phi_{j,n}\}_{n\in\mathbb{Z}^d}$ is an orthonormal basis of V_j for all $j \in \mathbb{Z}$. Define W_j to be the orthogonal complement of V_j in V_{j-1}:

$$V_{j-1} = V_j \oplus W_j. \tag{46}$$

Let $F_i^{[2]}$ $(0 \le i \le |\mathsf{M}| - 1)$ be the equivalent synthesis filters for the new reconstruction method REC-2, which in this case are simply the time-reversed versions of the analysis filters K_i. Note that $F_i^{[2]}$ are highpass filters. As in the wavelet filter bank, we associate to each of these filters a continuous function $\psi^{(i)}$ where

$$\psi^{(i)}(t) = |\mathsf{M}|^{1/2} \sum_{n\in\mathbb{Z}^d} f_i^{[2]}[n]\phi(\mathsf{M}t - n). \tag{47}$$

These functions also generate families of scaled and translated functions

$$\psi_{j,n}^{(i)} = |\mathsf{M}|^{-j/2}\psi^{(i)}(\mathsf{M}^{-j}t - n), \quad j \in \mathbb{Z}, n \in \mathbb{Z}^d. \tag{48}$$

The relationship between these functions and the computational procedure of the LP can be seen as follows. Suppose f is a function in V_{j-1}, then

$$f(t) = \sum_{n\in\mathbb{Z}^d} \underbrace{\langle f, \phi_{j-1,n}\rangle}_{c^{(j-1)}[n]} \phi_{j-1,n}(t). \tag{49}$$

Using the two-scale equations for ϕ and ψ, it is easy to verify that the inner products of f with functions at the next

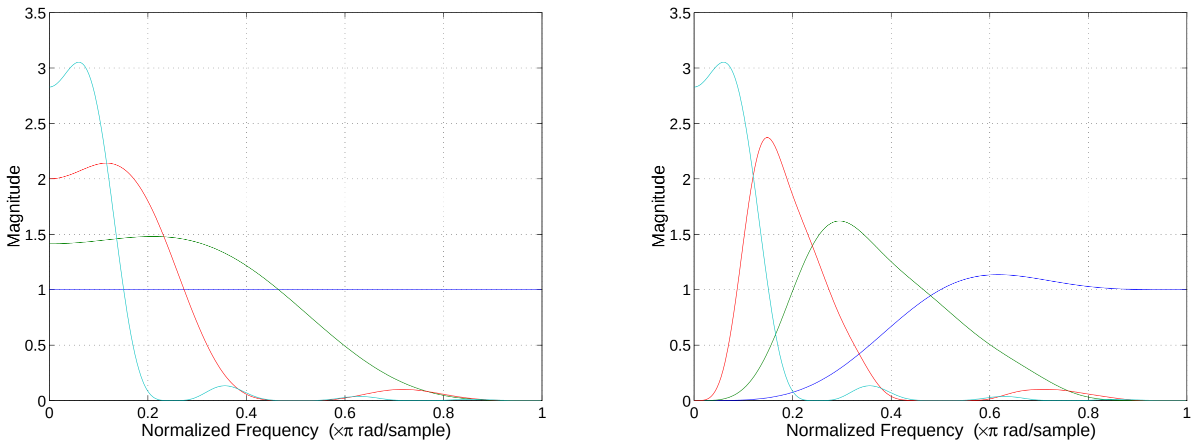

(a) (b)

Fig. 9. Frequency responses of the equivalent synthesis filters for the multi-level LP with "9-7" filters. (a) Usual reconstruction method REC-1. Note that all synthesis filters are lowpass. (b) New reconstruction method REC-2. Here, the synthesis filters are bandpass and match with the frequency regions of corresponding subbands, as expected. Consequently, REC-2 confines the influence of noise from the LP only in these localized bands.

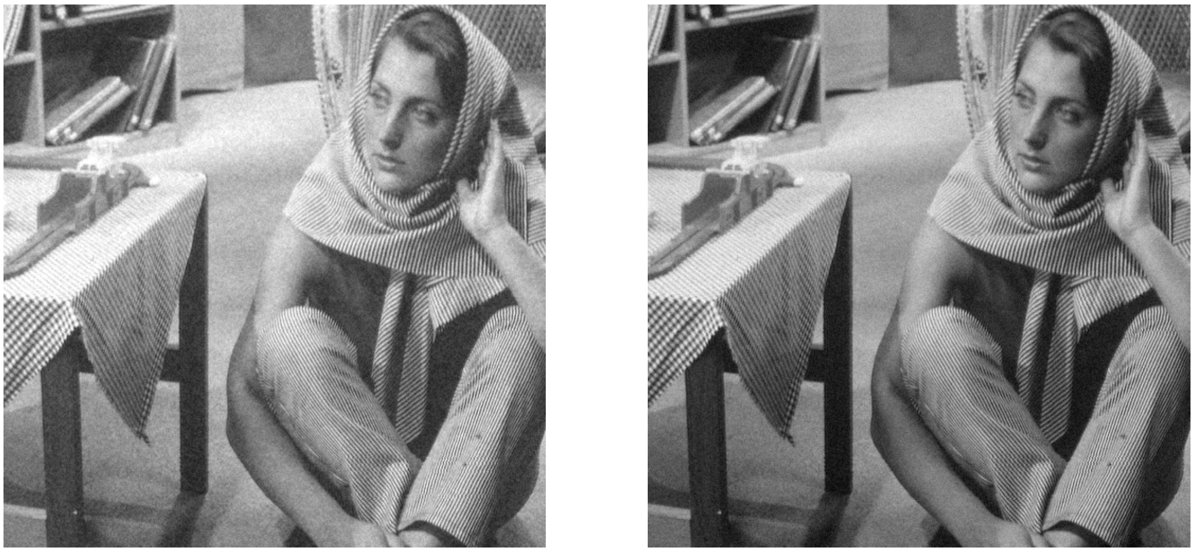

(a) (b)

Fig. 10. Reconstructions from the LP coefficients that are contaminated by an additive i.i.d. uniform noise in the interval $[0, 0.1]$ (the original pixel values are between 0 and 1). The LP is decomposed with 6 levels. (a) Usual reconstruction method REC-1: SNR = 6.28 dB. (b) New reconstruction method REC-2: SNR = 17.42 dB.

scale can be written as

$$c^{(j)}[n] = \langle f, \phi_{j,n} \rangle = \sum_{k \in \mathbb{Z}^d} c^{(j-1)}[k] g[k - \mathsf{M}n], \quad (50)$$

$$d_i^{(j)}[n] = \langle f, \psi_{j,n}^{(i)} \rangle = \sum_{k \in \mathbb{Z}^d} c^{(j-1)}[k] f_i^{[2]}[k - \mathsf{M}n]. \quad (51)$$

Therefore, $\{c^{(j)}[n],\ d^{(j)}[n]\}$ is exactly the output of the LP given the input sequence $c^{(j-1)}[n]$.

Theorem 5:

1) Suppose the LP with orthogonal filter generates an MRA. Then for a scale j, $\{\psi_{j,n}^{(i)}\}_{0 \le i \le |\mathsf{M}|-1,\ n \in \mathbb{Z}^d}$ is a tight frame of W_j. For all scales, $\{\psi_{j,n}^{(i)}\}_{0 \le i \le |\mathsf{M}|-1,\ j \in \mathbb{Z},\ n \in \mathbb{Z}^2}$ is a tight frame of $L^2(\mathbb{R}^d)$. In all cases, the frame bounds equal to 1.
2) Furthermore, suppose that $G(e^{j\omega})$ has an Lth-order zero at $2\pi \mathsf{M}^{-1} k_i,\ i = 1, \ldots, |\mathsf{M}| - 1$.[5] Then all polynomials of total degree less than L is reproduced by projection onto the space V_0 spanned by $\{\phi(t - n)\}_{n \in \mathbb{Z}^d}$, and the functions $\psi^{(i)}(t)$ have all moments up to order $L - 1$

[5]An Lth-order zero at a point means that all partial derivatives $\left(\frac{\partial}{\partial \omega_1}\right)^{p_1} \cdots \left(\frac{\partial}{\partial \omega_d}\right)^{p_d} G(e^{j\omega}),\ p_1 + \ldots + p_d < L$, equal to zero at that point.

vanish, i.e.

$$\int_{\mathbb{R}^d} t_1^{p_1} \dots t_d^{p_d} \psi^{(i)}(t) dt = 0, \tag{52}$$

for all $i = 0, \dots, |\mathsf{M}| - 1,\ p_1 + \dots + p_d \leq L - 1$.

Proof: See Appendix C ∎

With this, the family $\{\psi_{j,n}^{(i)}\}_{0 \leq i \leq |\mathsf{M}|-1,\ j \in \mathbb{Z},\ n \in \mathbb{Z}^2}$ is referred to as a tight wavelet frame or tight framelets [34]. For more general filters, with a similar setup, the LP filter bank in Figure 7 leads to a pair of wavelet frames – sometimes called bi-framelets [6] – generated by functions $\{\psi^{(i)}\}$ and $\{\tilde{\psi}^{(i)}\}$ for the analysis and synthesis sides, respectively. Figure 11 shows the 1-D bi-framelets derived from the iterated LP using "9-7" filters.

VII. Concluding Remarks

The Laplacian pyramid was studied using the theory of frames and oversampled filter banks. We proposed a new reconstruction algorithm for the LP based on projection, which is the pseudo inverse in certain cases. The new method presents an efficient filter bank, that leads to improvements over the usual method for reconstruction in the presence of noise. With Theorem 1, 3, and 4, we provided a complete characterization of tight frame, reconstruction using projection, and general reconstruction for the LP, respectively. Finally, we derived the continuous-domain frames associated with the iterated LP.

For practical applications, we recommend the use of the symmetric biorthogonal filters with sufficient accuracy numbers, such as the "9-7" pair for the LP, together with the proposed reconstruction method REC-2. The resulting LP exhibits excellent compression property for piecewise smooth signals, while having a simple structure, even in higher dimensions.

Appendix

A. Proof of Theorem 1

Suppose that the Laplacian pyramid uses orthogonal filters. A geometrical proof of the tight frame is already given in Section III-A. Alternatively, using $\mathsf{G}^*(z)\mathsf{G}(z) = 1$ and $\mathsf{H}(z) = \mathsf{G}^*(z)$ we can directly verify that

$$\mathsf{A}^*(z)\mathsf{A}(z) = \begin{pmatrix} \mathsf{H}^*(z) & \mathsf{I} - \mathsf{H}^*(z)\mathsf{G}^*(z) \end{pmatrix} \begin{pmatrix} \mathsf{H}(z) \\ \mathsf{I} - \mathsf{G}(z)\mathsf{H}(z) \end{pmatrix} = \mathsf{I}.$$

Now suppose that LP is a tight frame, or $\|\boldsymbol{c}\|^2 + \|\boldsymbol{d}\|^2 = \beta\|\boldsymbol{x}\|^2$ for all $\boldsymbol{x} \in l_2(\mathbb{Z}^d)$. Since H is a decimating operator, there exists an $\boldsymbol{x} \neq \boldsymbol{0}$ such that $\mathsf{H}\boldsymbol{x} = \boldsymbol{0}$. In this case, the output of the LP is $\boldsymbol{c} = \boldsymbol{0},\ \boldsymbol{d} = \boldsymbol{x}$. Hence the tight frame bound β must be 1.

So the tight frame condition for the LP becomes $\mathsf{A}^*(z)\mathsf{A}(z) = \mathsf{I}$. Expanding and grouping terms, this equation becomes

$$\mathsf{H}^*(z)[\mathsf{H}(z) - \mathsf{G}^*(z) + \mathsf{G}^*(z)\mathsf{G}(z)\mathsf{H}(z)] = \mathsf{G}(z)\mathsf{H}(z). \tag{53}$$

Let $\mathsf{K}(z) = \mathsf{H}(z) - \mathsf{G}^*(z) + \mathsf{G}^*(z)\mathsf{G}(z)\mathsf{H}(z)$. Note that $\mathsf{K}(z)$ is an $1 \times |\mathsf{M}|$ matrix, and denote $\mathsf{K}(z) = (K_0(z), \dots, K_{|\mathsf{M}|-1}(z))$. The key observation is that both sides of (53) are *outer products* of two column vectors of $|\mathsf{M}|$ components. Thus, (53) can be written as

$$K_i(z)\mathsf{H}^*(z) = H_i(z)\mathsf{G}(z), \quad \text{for} \quad i = 0, \dots, |\mathsf{M}| - 1.$$

If $H(z) = 0$, then (53) holds and we have a degenerated LP tight frame since $\boldsymbol{c} = \boldsymbol{0},\ \boldsymbol{d} = \boldsymbol{x}$ for all $\boldsymbol{x}$. Otherwise, there exists a polyphase component $H_i(z) \neq 0$, which implies $\mathsf{G}(z) = [K_i(z)/H_i(z)]\mathsf{H}^*(z) = \alpha(z)\mathsf{H}^*(z)$. Substitute this back to (53), it becomes

$$\begin{aligned} \alpha(z)\alpha(z^{-1})\mathsf{H}^*(z)\mathsf{H}(z)\mathsf{H}^*(z)\mathsf{H}(z) \\ = [\alpha(z) + \alpha(z^{-1}) - 1]\mathsf{H}^*(z)\mathsf{H}(z). \end{aligned} \tag{54}$$

Since $H(z) \neq 0$, it can be shown that $\mathsf{H}(z)$ has a right inverse $\bar{\mathsf{H}}(z)$, such that $\mathsf{H}(z)\bar{\mathsf{H}}(z) = 1$. Multiplying both sides of (54) with $\bar{\mathsf{H}}^*(z)$ on the left and $\bar{\mathsf{H}}(z)$ on the right, and noting that $\mathsf{G}(z) = \alpha(z)\mathsf{H}^*(z)$, we have equivalently $\mathsf{G}^*(z)\mathsf{G}(z) = \alpha(z) + \alpha(z^{-1}) - 1$.

B. Proof of Theorem 3

1. The transform matrix for the reconstruction algorithm in Figure 3 can be written as

$$\mathsf{S}_2 = \begin{pmatrix} \mathsf{G} & \mathsf{I} - \mathsf{G}\mathsf{H} \end{pmatrix} \tag{55}$$

From the expression for A in (4), we have $\mathsf{S}_2\mathsf{A} = \mathsf{I} - \mathsf{G}\mathsf{H} + (\mathsf{G}\mathsf{H})^2$. Therefore, S_2 is a left inverse of A if and only if $\mathsf{G}\mathsf{H} = (\mathsf{G}\mathsf{H})^2$ or $\mathsf{G}\mathsf{H}$ is a projector.

We note that H and G possess right and left inverses, respectively (which involves inverse filters of H and G). Thus the projection condition $\mathsf{G}\mathsf{H} = \mathsf{G}\mathsf{H}\mathsf{G}\mathsf{H}$ is equivalent to

$$\mathsf{H}\mathsf{G} = \mathsf{I} \quad \text{or} \quad \langle \tilde{h}[\cdot - \mathsf{M}k], g[\cdot - \mathsf{M}l] \rangle = \delta[k - l] \quad \forall k, l \in \mathbb{Z}^d. \tag{56}$$

Filters H and G satisfying (56) are said to be biorthogonal filters (with respect to the sampling matrix M). This proves part 1.

2. For part 2, we require additionally that S_2 is a pseudo inverse of A. From (13) this means that $\mathsf{A}^T\mathsf{A}\mathsf{S}_2 = \mathsf{A}^T$. Using the assumption that $\mathsf{H}\mathsf{G} = \mathsf{I}$, after some manipulations we have that

$$\mathsf{A}^T\mathsf{A}\mathsf{S}_2 = \begin{pmatrix} \mathsf{H}^T & (\mathsf{I} - \mathsf{G}\mathsf{H})(\mathsf{I} - \mathsf{H}^T\mathsf{G}^T) \end{pmatrix}$$

So the pseudo inverse condition is simplified to

$$(\mathsf{I} - \mathsf{G}\mathsf{H})(\mathsf{I} - \mathsf{H}^T\mathsf{G}^T) = (\mathsf{I} - \mathsf{G}\mathsf{H})^T \tag{57}$$

Notice that the left hand side of (57) is a symmetric matrix, thus it is the case for $(\mathsf{I} - \mathsf{G}\mathsf{H})^T$ and $\mathsf{G}\mathsf{H}$ as well. Therefore, $\mathsf{G}\mathsf{H}$ is an orthogonal projector, which proves the part 2.

C. Proof of Theorem 5

1. Let f be a function in W_j. This is equivalent to $f \in V_{j-1}$ and $f \perp V_j$. Therefore, f can be expanded by an orthonormal basis of V_{j-1} as in (49), and $c^{(j)}[n] = \langle f, \phi_{j,n} \rangle = 0$, for all $n \in \mathbb{Z}^d$.

Now suppose that f is analyzed via the LP as in (51). From Theorem 1, with orthogonal filters, the LP provides a tight frame with frame bounds equal 1, or $||c^{(j-1)}||^2 = ||c^{(j)}||^2 + \sum_{i=0}^{|\mathsf{M}|-1} ||d_i^{(j)}||^2$.

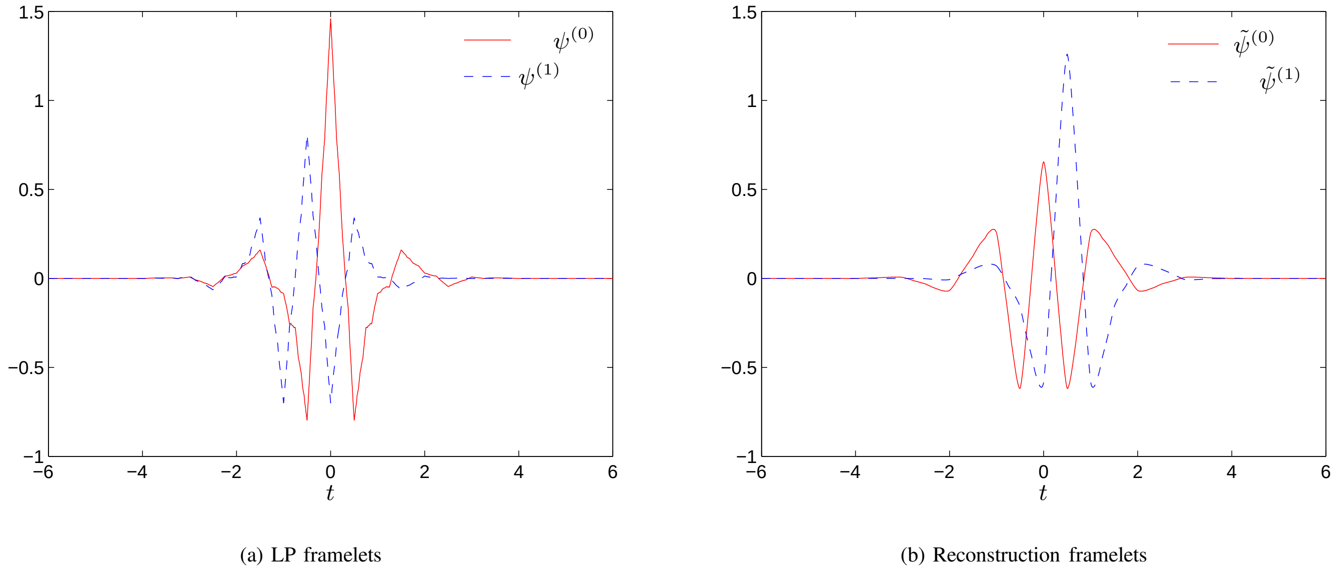

Fig. 11. Bi-frame from the LP with the "9-7" filters. (a) Analysis framelets. (b) Synthesis framelets using the new reconstruction method.

Consequently,

$$||f||^2 = ||c^{(j-1)}||^2 = \sum_{i=0}^{|\mathsf{M}|-1} ||d_i^{(j)}||^2 = \sum_{i=0}^{|\mathsf{M}|-1} \sum_{n\in\mathbb{Z}^d} |\langle f, \psi_{j,n}^{(i)}\rangle|^2,$$

which proves the tight frame condition for W_j. The result for $L^2(\mathbb{R}^d)$ immediately follows since the MRA conditions implies that

$$L^2(\mathbb{R}^d) = \bigoplus_{j\in\mathbb{Z}} W_j,$$

a decomposition of $L^2(\mathbb{R}^d)$ into mutual orthogonal subspaces.

2. For part 2, the first statement is the multivariate Strang-Fix conditions (see, for example, [38]). The second statement comes from the facts $\psi^{(i)}(t) \in W_0$ and $W_0 \perp V_0$.

Acknowledgments

This work was supported in part by a Ph.D. Fellowship from the Department of Communication Systems, EPFL. The authors would like to thank Prof. Michael Unser, Dr. Vivek Goyal, and Jianping Zhou for their helpful comments and suggestions.

References

[1] P. J. Burt and E. H. Adelson, "The Laplacian pyramid as a compact image code," *IEEE Trans. Commun.*, vol. 31, no. 4, pp. 532–540, April 1983.

[2] A. Rosenfeld, Ed., *Multiresolution Image Processing and Analysis*. New York: Springer-Verlag, 1984.

[3] R. H. Bamberger and M. J. T. Smith, "A filter bank for the directional decomposition of images: Theory and design," *IEEE Trans. Signal Proc.*, vol. 40, no. 4, pp. 882–893, April 1992.

[4] M. N. Do and M. Vetterli, "Pyramidal directional filter banks and curvelets," in *Proc. IEEE Int. Conf. on Image Proc.*, Thessaloniki, Greece, Oct. 2001.

[5] ——, "Contourlets," in *Beyond Wavelets*, G. V. Welland, Ed. New York: Academic Press, 2003, to appear, `http://www.ifp.uiuc.edu/~minhdo/publications`.

[6] I. Daubechies, B. Han, A. Ron, and Z. Shen, "Framelets: MRA-based constructions of wavelet frames," 2001, preprint, `ftp://ftp.cs.wisc.edu/Approx/dhrs.ps`.

[7] C. K. Chui, W. He, and J. Stöckler, "Compactly supported tight and sibling frames with maximum vanishing moments," Department of Statistics, Stanford University, Tech. Rep. 2001-04, 2001, `http://www-stat.stanford.edu/research/`.

[8] I. W. Selesnick, "The double density DWT," in *Wavelets in signal and image analysis: from theory to practice*, A. Petrosian and F. G. Meyer, Eds. Kluwer, 2001, `http://taco.poly.edu/selesi/`.

[9] J. Kovačević, P. L. Dragotti, and V. K. Goyal, "Filter bank frame expansions with erasures," *IEEE Trans. Inform. Th.*, vol. 48, no. 6, pp. 1439–1450, Jun. 2002.

[10] P. P. Vaidyanathan, *Multirate Systems and Filter Banks*. Englewood Cliffs, NJ: Prentice-Hall, 1993.

[11] M. Vetterli and J. Kovačević, *Wavelets and Subband Coding*. Englewood Cliffs, NJ: Prentice-Hall, 1995.

[12] R. J. Duffin and A. C. Schaeffer, "A class of nonharmonic Fourier series," *Trans. Amer. Math. Soc.*, vol. 72, pp. 341–366, 1952.

[13] I. Daubechies, "The wavelet transform, time-frequency localization and signal analysis," *IEEE Trans. Inform. Th.*, vol. 36, no. 5, pp. 961–1005, September 1990.

[14] ——, *Ten Lectures on Wavelets*. Philadelphia, PA: SIAM, 1992.

[15] A. Aldroubi, "Portraits of frames," *Proc. Amer. Math. Soc.*, vol. 123, pp. 1661–1668, 1995.

[16] S. Mallat, *A Wavelet Tour of Signal Processing*, 2nd ed. Academic Press, 1999.

[17] R. A. Horn and C. R. Johnson, *Matrix Analysis*. Cambridge University Press, 1985.

[18] Z. Cvetković and M. Vetterli, "Oversampled filter banks," *IEEE Trans. Signal Proc.*, vol. 46, pp. 1245 –1255, May 1998.

[19] V. K. Goyal, J. Kovačević, and J. A. Kelner, "Quantized frame expansions with erasures," *Applied and Computational Harmonic Analysis*, vol. 10, no. 3, pp. 203–233, May 2001.

[20] H. Bölcskei and F. Hlawatsch, "Noise reduction in oversampled filter banks using predictive quantization," *IEEE Trans. Inform. Th.*, vol. 47, no. 1, pp. 155–172, Jan. 2001.

[21] G. Karlsson and M. Vetterli, "Theory of two - dimensional multirate filter banks," *IEEE Trans. Acoust., Speech, and Signal Proc.*, vol. 38, no. 6, pp. 925–937, June 1990.

[22] J. Kovačević and M. Vetterli, "Nonseparable two- and three-dimensional wavelets," *IEEE Trans. Signal Proc.*, vol. 43, no. 5, pp. 1269–1273, May 1995.

[23] M. Unser, "An improved least squares Laplacian pyramid for image compression," *Signal Proc.*, vol. 27, pp. 187–203, May 1992.

[24] A. Cohen, I. Daubechies, and J.-C. Feauveau, "Biorthogonal bases of

compactly supported wavelets," *Commun. on Pure and Appl. Math.*, vol. 45, pp. 485–560, 1992.
[25] M. Vetterli and C. Herley, "Wavelets and filter banks: Theory and design," *IEEE Trans. Signal Proc.*, vol. 40, no. 9, pp. 2207–2232, September 1992.
[26] M. Antonini, M. Barlaud, P. Mathieu, and I. Daubechies, "Image coding using wavelet transform," *IEEE Trans. Image Proc.*, vol. 1, no. 2, pp. 205–220, April 1992.
[27] M. Unser and A. Aldroubi, "A general sampling theory for non-ideal acquisition devices," *IEEE Trans. Signal Proc.*, pp. 2915–2925, 1994.
[28] K. Ramchandran, A. Ortega, and M. Vetterli, "Bit allocation for dependent quantization with applications to multiresolution and MPEG video coders," *IEEE Trans. Image Proc.*, vol. 3, no. 5, pp. 533–545, September 1994.
[29] V. K. Goyal, M. Vetterli, and N. T. Thao, "Quantized overcomplete expansions in $\mathbb{R}^n$: Analysis, synthesis and algorithms," *IEEE Trans. Inform. Th.*, vol. 44, no. 1, pp. 16–31, Jan. 1998.
[30] Y. Shoham and A. Gersho, "Efficient bit allocation for an arbitrary set of quantizers," *IEEE Trans. Acoust., Speech, and Signal Proc.*, vol. 36, no. 9, pp. 1445–1453, September 1988.
[31] G. Strang and T. Nguyen, *Wavelets and Filter Banks*. Boston: Wellesley Cambridge Press, 1996.
[32] H. Bölcskei, F. Hlawatsch, and H. G. Feichtinger, "Frame-theoretic analysis of oversampled filter banks," *IEEE Trans. Signal Proc.*, vol. 46, pp. 3256–3268, Dec. 1998.
[33] E. P. Simoncelli and E. H. Adelson, "Subband transforms," in *Subband Image Coding*, J. W. Woods, Ed. Boston, MA: Kluwer Academic Publishers, Inc., 1991, pp. 143–192.
[34] A. Ron and Z. Shen, "Affine systems in $L_2(\mathbb{R}^d)$: The analysis of the analysis operator," *J. Functional Anal.*, no. 148, pp. 408–447, 1997.
[35] J. Benedetto and S. D. Li, "The theory of multiresolution analysis frames and applications to filter banks," *Journal of Appl. and Comput. Harmonic Analysis*, vol. 5, no. 4, pp. 389–427, 1998.
[36] S. Mallat, "Multiresolution approximations and wavelet orthonormal bases of $L_2(R)$," *Trans. Amer. Math. Soc.*, vol. 315, pp. 69–87, September 1989.
[37] Y. Meyer, *Wavelets and Operators*, ser. Advanced mathematics. Cambridge University Press, 1992.
[38] A. Cohen, K. Gröchenig, and L. F. Villemoes, "Regularity of multivariate refinable functions," *Constr. Approx.*, vol. 15, pp. 241–255, 1999.

PLACE PHOTO HERE

Minh N. Do was born in Thanh Hoa, Vietnam, in 1974. He received the B.Eng. degree in computer engineering (with first class honors) from the University of Canberra, Australia, in 1997, and the Dr.Sci. degree in communication systems from the Swiss Federal Institute of Technology Lausanne (EPFL), Switzerland, in 2001.

Since 2002, he has been an Assistant Professor with the Department of Electrical and Computer Engineering and a Research Assistant Professor with the Coordinated Science Laboratory and the Beckman Institute, University of Illinois at Urbana-Champaign. His research interests include wavelets and harmonic analysis, multirate systems, image and multidimensional signal processing, and visual information representation and retrieval.

Dr. Do received a Silver Medal from the 32nd International Mathematical Olympiad in Sweden (1991), a University Medal from the University of Canberra (1997), the best doctoral thesis award from the Swiss Federal Institute of Technology Lausanne (2001), and a CAREER award from the National Science Foundation (2003).

PLACE PHOTO HERE

Martin Vetterli received the Dipl. El.-Ing. degree from ETH Zürich (ETHZ), Switzerland, in 1981, the MS degree from Stanford University in 1982, and the Doctorat ès Science degree from EPF Lausanne (EPFL), Switzerland, in 1986.

He was a Research Assistant at Stanford and EPFL, and has worked for Siemens and AT&T Bell Laboratories. In 1986, he joined Columbia University in New York where he was last an Associate Professor of Electrical Engineering and co-director of the Image and Advanced Television Laboratory. In 1993, he joined the University of California at Berkeley where he was a Professor in the Dept. of Electrical Engineering and Computer Sciences until 1997, and holds now Adjunct Professor position. Since 1995, he is a Professor of Communication Systems at EPF Lausanne, Switzerland, where he chaired the Communications Systems Division (1996/97), and heads of the Audio-Visual Communications Laboratory. He held visiting positions at ETHZ (1990) and Stanford (1998).

He is a fellow of the IEEE, a member of SIAM, and was the Area Editor for Speech, Image, Video, and Signal Processing of the IEEE Transactions on Communications. He is also on the editorial boards of Annals of Telecommunications, Applied and Computational Harmonic Analysis and The Journal of Fourier Analysis and Applications.

He received the Best Paper Award of EURASIP in 1984 for his paper on multidimensional subband coding, the Research Prize of the Brown Bovery Corporation (Switzerland) in 1986 for his doctoral thesis, the IEEE Signal Processing Society's Senior Award in 1991 and in 1996 (for papers with D.LeGall and K.Ramchandran, respectively), and he is a IEEE Signal Processing Distinguished lecturer in 1999. He received the Swiss National Latsis Prize in 1996 and the SPIE Presidential award in 1999. He is a member of the Swiss Council on Science and Technology.

He was a plenary speaker at various conferences (e.g. 1992 IEEE ICASSP) and is the co-author, with J.Kovacevic, of the book **Wavelets and Subband Coding** (Prentice-Hall, 1995). He has published about 85 journal papers on a variety of topics in signal and image processing and holds 5 patents.

His research interests include wavelets, multirate signal processing, computational complexity, signal processing for telecommunications, digital video processing and compression and wireless video communications.